International Journal of Biological Macromolecules 209 (2022) 801–813

Contents lists available at ScienceDirect

International Journal of Biological Macromolecules

journal homepage: www.elsevier.com/locate/ijbiomac

Highly efficient, processive and multifunctional recombinant endoglucanase *Rf*GH5_4 from *Ruminococcus flavefaciens* FD-1 v3 for recycling lignocellulosic plant biomasses

Parmeshwar Vitthal Gavande [a], Priyanka Nath [a], Krishan Kumar [a], Nazneen Ahmed [a], Carlos M.G.A. Fontes [b,c], Arun Goyal [a,*]

[a] *Department of Biosciences and Bioengineering, Carbohydrate Enzyme Biotechnology Laboratory, Indian Institute of Technology Guwahati, Guwahati, Assam 781039, India*

[b] *CIISA - Faculdade de Medicina Veterinária, Universidade de Lisboa, Avenida da Universidade Técnica, 1300-477 Lisbon, Portugal*

[c] *NZYTech – Genes & Enzymes, Estrada do Paço do Lumiar, Campus do Lumiar, Edifício, Lisbon, Portugal*

ARTICLE INFO

Keywords:
Multifunctional
Processive
Endoglucanase

ABSTRACT

Gene encoding endoglucanase, *Rf*GH5_4 from *R. flavefaciens* FD-1 v3 was cloned, expressed in *Escherichia coli* BL21(DE3) cells and purified. *Rf*GH5_4 showed molecular size 41 kDa and maximum activity at pH 5.5 and 55 °C. It was stable between pH 5.0–8.0, retaining 85% activity and between 5 °C–45 °C, retaining 75% activity, after 60 min. *Rf*GH5_4 displayed maximum activity (U/mg) against barley β-D-glucan (665) followed by carboxymethyl cellulose (450), xyloglucan (343), konjac glucomannan (285), phosphoric acid swollen cellulose (86), beechwood xylan (21.7) and carob galactomannan (16), thereby displaying the multi-functionality. Catalytic efficiency ($mL.mg^{-1}\ s^{-1}$) of *Rf*GH5_4 against carboxymethyl cellulose (146) and konjac glucomannan (529) was significantly high. TLC and MALDI-TOF-MS analyses of *Rf*GH5_4 treated hydrolysates of cellulosic and hemicellulosic polysaccharides displayed oligosaccharides of degree of polymerization (DP) between DP2-DP11. TLC, HPLC and Processivity-Index analyses revealed *Rf*GH5_4 to be a processive endoglucanase as initially, for 30 min it hydrolysed cellulose to cellotetraose followed by persistent release of cellotriose and cellobiose. *Rf*GH5_4 yielded sufficiently high Total Reducing Sugar (TRS, mg/g) from saccharification of alkali pre-treated sorghum (72), finger millet (62), sugarcane bagasse (38) and cotton (27) in a 48 h saccharification reaction. Thus, *Rf*GH5_4 can be considered as a potential endoglucanase for renewable energy applications.

1. Introduction

Cellulose is the most abundant polysaccharide on earth, primarily present in the plant biomass [1]. It is an unbranched polysaccharide made up of glucose units linked by β-1,4-linkage. Cellulose can be hydrolyzed to monosaccharide (glucose) and subsequently converted to bioethanol [2]. Therefore, cellulosic plant biomass is seen as a significant renewable energy source. Cellulose is hydrolyzed synergistically to cellooligosaccharides, cellobiose and glucose by various bacterial or fungal cellulase enzymes. These are namely, endoglucanase (EC 3.2.1.4), exoglucanase (EC 3.2.1.91) and β-glucosidase (EC 3.2.1.21). Endoglucanase randomly hydrolyzes cellulose chain to cellooligosaccharides, whereas exoglucanase produces cellobiose entities [3]. The produced cellooligosaccharides and cellobiose are then hydrolyzed to D-glucose by β-glucosidase [4]. Cellulases are distributed over 15 different glycoside hydrolase (GH) families of Carbohydrate Active Enzyme (CAZy) database (http://www.cazy.org). The classification is based on the amino acid sequence of enzyme and function [5]. The glycoside hydrolase family 5 (GH5) is one of the largest GH families. The subfamily 4 (GH5_4) of family GH5 is known for cellulases showing broad substrate specificity. The enzymes from the subfamily GH5_4 can display multifunctional activities by acting as endoglucanase (EC 3.2.1.4), lichenase (EC 3.2.1.73), xylanase (EC 3.2.1.8) and xyloglucanase (EC 3.2.1.151) [6].

The conversion of lignocellulosic biomass to bioethanol currently faces a bottleneck which is the unavailability of catalytically efficient and stable endoglucanases. Moreover, the lignocellulosic biomass contains hemicellulose along with the cellulose. It is highly advantageous if

* Corresponding author at: Department of Biosciences and Bioengineering, Indian Institute of Technology Guwahati, Guwahati 781039, Assam, India.
E-mail address: arungoyl@iitg.ac.in (A. Goyal).

https://doi.org/10.1016/j.ijbiomac.2022.04.059
Received 8 February 2022; Received in revised form 18 March 2022; Accepted 8 April 2022
Available online 12 April 2022

the endoglucanase hydrolyzes more than one cellulosic and hemicellulosic substrate. Recently, an alkali stable bifunctional β-glucanase, *Pgl5A* of subfamily 4 of family GH5 from *Paenibacillus* sp. S09 was characterized that showed 94.5 U/mg of specific activity on tamarind xyloglucan, however, its activity against CMC-Na was negligible, 0.5 U/mg [7]. Another multifunctional alkali tolerant family GH5 endoglucanase, *Thrcel5A*, from *Thermoactinospora rubra YIM 77501T* was reported to show 85.7 U/mg specific activity against CMC-Na and 22.9 U/mg against beechwood xylan, respectively at the optimum pH of 8.5 and 60 °C [8]. An endoglucanase *SoCel5* from bacterium *Stegonsporium opalus* from family GH5 showed a specific activity of 350 U/mg and catalytic efficiency of 77 $mL.mg^{-1}$ s^{-1} on carboxymethyl cellulose (CMC—Na) at pH 6 and 60 °C [9]. Another endoglucanase, *CelR5* of family GH5 from rhizosphere metagenomic library showed the specific activity of 15 U/mg and k_{cat} of 9.7 s^{-1} against CMC-Na [10]. Moreover, a thermophilic microbial consortium developed on rice straw from vermicompost reported only 20 U/mg of the endoglucanase activity [11]. However, the lignocellulose deconstruction demands more efficient endoglucanases with higher catalytic efficiency, having a broad range of substrate specificity, pH stability and thermostability. Multifunctional and efficient endoglucanases could reduce the cost of bioethanol production, increase the productivity, thereby by making the bioethanol industry economically sustainable. The aim of this study was to explore a new endoglucanase, *Rf*GH_4 from a ruminant gut bacterium *Ruminococcus flavefaciens* FD-1 v3 for lignocellulosic biomass conversion.

Inhabitant bacteria of herbivorous rumen have been facing cellulosic pressure since time immemorial. These rumen loving microorganisms have evolved efficient machinery, i.e., the cellulosomes, to deconstruct the cellulose. *Ruminococcus flavefaciens* FD-1 v3 is an anaerobic, mesophilic and a Gram-positive bacterium. FD-1 v3 strain of *R. flavefaciens* was isolated from bolus earlier [12]. *R. flavefaciens* resides in the intestine of monogastric mammalian herbivores as one of its natural microbiome [13]. It is the most populated cellulolytic inhabitant of the animal rumen. Genome sequencing analysis of *R. flavefaciens* FD-1 v3 uncovered a vast array of cellulosomal genes. These are putatively considered versatile for the efficient degradation of lignocellulose [14]. A putative multienzyme complex (cellulosome) of family GH5 from *R. flavefaciens* FD-1 v3, named as *Rf*$GH5_{1/2}$, consists of an endoglucanase module (*Rf*GH5_4) at N-terminal domain followed by family 80 Carbohydrate Binding Module (CBM80), a catalytic *endo*-mannanase module (*Rf*GH5_7) and a dockerin at the C-terminal [13]. The module, *Rf*GH5_7 was recently characterized as an efficient endomannanase [15]. In the present investigation, the role of the catalytic module, *Rf*GH5_4 of *Rf*$GH5_{1/2}$ has been investigated. The gene encoding a putative endoglucanase, *Rf*GH5_4 from *R. flavefaciens* FD-1 v3 (GenBank Accession Number WP_009984467.1) was cloned and expressed in *E. coli* BL-21 expression system. The purified enzyme, *Rf*GH5_4 was biochemically characterized and its application in the saccharification of various lignocellulosic biomasses was investigated to explore for bioethanol production.

This study describes the biochemical and kinetic parameters of a multifunctional endoglucanase (*Rf*GH_4) such as pH, temperature, stability and catalytic efficiency. These properties play a pivotal role in evaluating the importance of a cellulase in the renewable energy sector. Based on the unique properties, *Rf*GH5_4 is prospected as a potent cellulase for lignocellulosic bioethanol production. The efficiency of *Rf*GH5_4 for lignocellulose biomass hydrolysis was tested by saccharification of six different alkali pre-treated biomasses namely cotton main stalk, cotton small branches, sorghum stalk, sugarcane bagasse, finger millet stalk and maize leaves. The hydrolysis of hemicellulosic chains such as xyloglucan and glucomannan by multifunctional *Rf*GH5_4 would further increase the accessibility of cellulose content of lignocellulose. Moreover, *Rf*GH5_4 was found to be a processive endoglucanase thus releasing the cellobiose, which will reduce the need of cellobiohydrolase during the saccharification of biomass thereby helping in reducing the cost of saccharification process. In addition, *Rf*GH5_4 was found remarkably stable in ethanol making it a suitable endoglucanase for Simultaneous Saccharification and Fermentation (SSF) process for bioethanol production.

2. Materials and methods

2.1. Bacterial strains, vectors

pHTP1, the bacterial expression vector, was received from *Nzytech genes and enzymes* Pvt. Ltd., Lisbon, Portugal. *E. coli* TOP10 competent cells were used to amplify recombinant pHTP1 vector containing the gene encoding *Rf*GH5_4. *E. coli* BL21 (DE3) (Novagen) cells were used for the expression of the *Rf*GH5_4 enzyme.

2.2. The substrates, chemicals and kits

Barley β-D-Glucan, sodium salt of carboxymethyl-cellulose (CMC—Na), avicel, birchwood xylan, konjac glucomannan, carob galactomannan, D-glucose and dihydroxybenzoic acid (DHB) were procured from Sigma-Aldrich Co. LLC., USA. Isopropyl-β-D thiogalactopyranoside (IPTG), kanamycin, hydroxyethyl cellulose (HEC), lichenan were also purchased from Sigma-Aldrich Co. LLC., USA. Xyloglucan was purchased from Megazyme International, Ireland. Beechwood xylan was purchased from SRL India Pvt. Ltd. Cellulose powder, ethylene diamine tetraacetic acid (EDTA), ethylene glycol tetraacetic acid (EGTA), 2-(*N*-morpholino) ethane sulfonic acid (MES) buffer and protein dialysis tube (pore size, 12–14 kDa) were purchased from Hi-Media Laboratories Pvt. Ltd., India. Phosphoric Acid Swollen Cellulose (PASC), also known as Regenerated Amorphous Cellulose (RAC), was prepared from avicel. The NZYEasy pHTP1 cloning and expression kit from Nzytech genes and enzymes Ltd., Lisbon, Portugal was used for cloning. A thin layer chromatography plate (TLC Silica gel 60 F_{254}, 20 × 20 cm) was purchased from Merck KGaA, Darmstadt, Germany.

2.3. Molecular architecture of RfGH5_4

The sequence of a multienzyme complex of a family GH5 from *R. flavefaciens* FD-1 v3, named as *Rf*$GH5_{1/2}$ which contains the putative catalytic module, *Rf*GH5_4, was taken from the CAZy database having GenBank accession number WP_009984467.1. The amino acid sequence of *Rf*$GH5_{1/2}$ was analysed for the conserved domains and homologs by using the conserved sequence database, NCBI-CDD (http://www.ncbi.nlm.nih.gov/cdd) and NCBI-blast analysis [16], respectively. The signal peptide was located in the *Rf*$GH5_{1/2}$ sequence with the assistance of the SignalP 3.0 server (http://www.cbs.dtu.dk/services/SignalP).

2.4. Gene amplification and cloning

The gene encoding *Rf*GH5_4 was amplified from the genomic DNA of *R. flavefaciens* FD-1 v3 by PCR using an NZYProof DNA polymerase (Nzytech genes and enzymes Ltd., Lisbon, Portugal) kit following the manufacturer's protocol. The forward and reverse primers used for PCR were: F-5'-TCAGCAAGGGCTGAGGGCTTCCAACATGACCGCAAG-3′, R-5′- TCAGCGGAAGCTGAGGTTATACTCCGAGTACTTCCATC-3′, respectively. PCR amplification was performed by the initial denaturing at 95 °C for 3 min followed by 30 cycles of denaturation at 95 °C for 30 s, annealing at 50 °C for 30 s, extension at 72 °C for 60 s and the final extension at 72 °C for 10 min. The amplified gene encoding *Rf*GH5_4 enzyme was cloned into the linearized pHTP1 vector by restriction endonuclease and ligase independent and temperature dependent directional cloning using NZYEasy cloning and expression kit (MB282) by following the manufacturer's protocol. The pHTP1 vector available with the kit containing the complementary overhangs, was added in the PCR product amplified by using the primers with appropriate 5′ extensions (Underlined in aforementioned primers' sequence). Through base-

pair complementation, the gene of interest was joined in the vector using NZYEasy enzyme mix. The cloned gene encoding *Rf*GH5_4 was sequenced to confirm that no mutations generated during the amplification process. His_6-tag was incorporated at the N-terminal of *Rf*GH5_4 by the pHTP1 vector. The recombinant plasmid containing pHTP1 vector and the gene encoding *Rf*GH5_4 was transformed using *E. coli* TOP10 competent cells for plasmid amplification.

2.5. Expression and purification of RfGH5_4

The *E. coli* BL21 (DE3) cells were transformed with recombinant pHTP1 plasmid, containing the gene encoding *Rf*GH5_4. The expression and purification of *Rf*GH5_4 were performed as per the protocol given in the literature [17]. Briefly, the expression of *Rf*GH5_4 by *E. coli* BL21 (DE3) cells was carried out in 400 mL LB medium containing 50 μg/mL kanamycin and 1 mM IPTG by incubating at 24 °C. The cell pellet was resuspended in the 5 mL 20 mM sodium phosphate buffer (pH 7.0), containing 50 mM imidazole and 300 mM NaCl and subjected to sonication. The purification of *Rf*GH5_4 was performed by Immobilized Metal Ion Affinity Chromatography (IMAC). The cell free extract obtained by centrifugation of sonicated pellet was loaded onto an Ni^{2+} ions charged IMAC column (1.0 mL HiTrap, GE Healthcare, USA). The His_6-tagged *Rf*GH5_4 protein was eluted by 5 mL elution buffer (20 mM sodium phosphate, pH 7.0, 300 mM NaCl, 300 mM imidazole). The eluted *Rf*GH5_4 protein was dialyzed against 20 mM sodium phosphate buffer (pH 7.0) and run through the sodium dodecyl sulfate-polyacrylamide gel electrophoresis (SDS-PAGE) on a 12% (w/v) gel to check its purity. The gel was stained with Coomassie Brilliant Blue R-250 to observe the protein bands. The Bradford method was used for estimating the concentration of purified protein by using Bovine Serum Albumin (BSA) as the standard.

2.6. Substrate specificity of RfGH5_4

The enzyme activity of *Rf*GH5_4 was determined against different carbohydrate polymers like β-1,4-glucans (CMC—Na, HEC, PASC, avicel and cellulose powder), mixed β-1,3;1,4 linked glucans (barley β-D-glucan and lichenan), tamarind xyloglucan, konjac glucomannan, carob galactomannan and xylans (beechwood and birchwood xylan). The reaction mixture (100 μL) consisted of 1% (w/v) of the polysaccharide as the substrate dissolved in 20 mM citrate-phosphate buffer (pH 5.5) and 10 μL purified *Rf*GH5_4 enzyme (5 μg/mL). The reaction mixture was incubated at 55 °C for an optimized time period of 2 min. For avicel and cellulose powder, the reaction was carried out at 30 °C with the rotation of 200 rpm for 2 h as reported earlier [18]. The temperature 30 °C was selected for the assay of avicel and cellulose powder since the enzyme, *Rf*GH5_4 is not thermally stable at 55 °C when incubated for more than 10 min. The released reducing sugar was quantified by the methods of Nelson [19] and Somogyi [20] for calculating the enzyme activity of *Rf*GH5_4. D-glucose was employed as a standard to calculate the enzyme activity of *Rf*GH5_4. One unit of specific activity was defined as the μmol of glucose produced from the substrate per minute per mg of the enzyme (μmol/min/mg) under the optimized reaction conditions. All the assays were performed in triplicate sets.

2.7. Biochemical characterization of RfGH5_4

The effect of pH on the enzyme activity of *Rf*GH5_4 was studied by using 20 mM buffers of the following pH range: sodium citrate-phosphate (pH 3.0–7.0), sodium phosphate (pH 5.8–8.0). The reaction mixture (100 μL) of different pHs containing 1% (w/v) CMC-Na and 10 μL (5 μg/mL) of the enzyme was incubated at 55 °C for 2 min. The released reducing sugar was estimated as described in Section 2.6 and the enzyme activity was calculated. The effect of temperature on the activity of *Rf*GH5_4 was studied by incubating (2 min) the 100 μL reaction mixture in 20 mM citrate-phosphate buffer (pH 5.5) and the temperature range in between 30 °C and 80 °C. The pH stability of *Rf*GH5_4 was performed by incubating the 100 μL of enzyme at various pH in the buffers: 20 mM sodium citrate-phosphate (pH 3.0–7.0), 20 mM sodium phosphate (pH 5.8–8.0), 20 mM MES (pH 5.5–6.7) and 20 mM Tris-Cl (pH 7.5–9.0), at 30 °C for 60 min. 10 μL aliquot of the enzyme was taken in a 100 μL reaction mixture and was assayed at an optimized reaction pH (5.5) and temperature (55 °C) for 2 min. The thermostability of *Rf*GH5_4 was analysed by incubating the 100 μL of the enzyme (5 μg/mL) at different temperatures (5 °C -70 °C) for 60 min. 10 μL of this incubated enzyme was used for the enzyme assay in a 100 μL reaction mixture as mentioned earlier to calculate the specific activity at optimum reaction pH (5.5) and temperature (55 °C). The highest activity obtained in pH stability and thermostability experiments was considered 100% to calculate the relative pH stability and thermostability of *Rf*GH5_4, respectively. All the assays were performed in triplicate sets.

2.8. Effect of metal ions, chelating agents and additive on RfGH5_4 activity

The enzyme, *Rf*GH5_4 (5 μg/mL final concentration) in a 100 μL reaction mixture volume containing 1%, w/v CMC-Na in 20 mM citrate-phosphate buffer (pH 5.5) with 10 mM concentration of metal ions or additives/chelating agents (EDTA, EGTA, SDS, Urea or guanidine hydrochloride, etc.) was incubated at 55 °C, and the reducing sugar was estimated by following the protocol reported earlier [21]. The metal ions used for the assay were: Mg^{2+} ($MgCl_2$), Ca^{2+} ($CaCl_2$), Na^{+} (NaCl), K^{+} (KCl), Mn^{2+} ($MnCl_2$), Li^{+} (LiCl), Co^{2+} ($CoCl_2$) and Ni^{2+} ($NiSO_4$), Fe^{2+} ($FeSO_4$), Zn^{2+} ($ZnCl_2$), and Cu^{2+} ($CuSO_4$). The effect of urea (100 mM), guanidine hydrochloride (10 mM) and SDS (0.1%, w/v), Triton X-100 (0.5%, v/v), Tween-80 (1%, v/v), dimethyl sulfoxide (DMSO, 1%, v/v), glycerol (10%, v/v), on *Rf*GH5_4 enzyme activity was also studied. A blank for each reaction containing 1% (w/v) CMC-Na without any additive was used. Ethanol tolerance of *Rf*GH5_4 was studied by incubating it with ethanol at 0, 1, 4, 7 and 20% (v/v) in 20 mM sodium-phosphate buffer, pH 6.0 at 30 °C for 96 h. The enzyme activity of *Rf*GH5_4 under optimal reaction conditions, without any additive was considered as 100%, to calculate the relative activity of enzyme with additive.

2.9. Protein melting curve of RfGH5_4

The temperature at which *Rf*GH5_4 melts was deduced by subjecting 50 μg/mL of enzyme in a freshly prepared 20 mM MES buffer, pH 5.5 to increasing temperature with an increment of 1 °C per min from 25 °C to 100 °C on a UV–visible spectrophotometer (Varian, Cary 100 Bio) attached with the Peltier temperature controller. The absorbance change at 280 nm (A_{280}) was recorded at varying temperatures, thereby generating a curve of absorbance against the temperature. The effect of 10 mM K^{+} and Ca^{2+} ions on the stability and melting temperature of *Rf*GH5_4 was also analysed. An independent experiment was carried out by incubating the enzyme at different temperatures in the presence of 10 mM EDTA to examine its effect on the enzyme structure.

2.10. Kinetic parameter analysis of RfGH5_4 against polysaccharides

The kinetic parameters of *Rf*GH5_4 were evaluated by the Michaelis-Menten equation under steady-state conditions using different substrates. The enzyme (5 μg/mL) was incubated with different concentration of carbohydrate substrates, namely, barley β-D-glucan, CMC—Na, tamarind xyloglucan, lichenan, and konjac glucomannan in a 100 μL reaction volume under 20 mM citrate-phosphate buffer (pH 5.5) at 55 °C temperature for 2 min. The equivalent concentration of substrates was taken as blank and all the reactions were performed in triplicates. The enzyme activity was calculated as mentioned in Section 2.6. A double-reciprocal (Lineweaver-Burk) plot [22] of the Michaelis-Menten equation [23] was generated by using GraphPad Prism 6 to determine the kinetic parameters, namely K_m, V_{max}, turnover number

(k_{cat}), and catalytic efficiency (k_{cat} /K_m, mL.mg^{-1} s^{-1}).

2.11. Catalytic mechanism of RfGH5_4

The hydrolyzed CMC-Na products by *Rf*GH5_4 were analysed using TLC to unveil the enzyme's mode of action by following the standard protocol as reported earlier [2]. 100 μL reaction mixture containing 90 μL of 1% (w/v) CMC-Na dissolved in 20 mM citrate-phosphate buffer (pH 5.5) and 10 μL of *Rf*GH5_4 (50 μg/mL) was incubated at 30 °C for different time intervals (1, 2, 5, 10, 15, 30, 45 and 60 min as well as 2, 4, 6, 12 and 24 h). 1 μL of each hydrolysate and 0.5 μL (10 mg/mL) mixture of standards (D-glucose, cellobiose, cellotriose and cellotetraose) were loaded on the TLC plate. The chromatogram was developed as reported by Kumar et al. [2]. 10 μL of the hydrolysate from each reaction was subjected to estimation of reducing sugar using the method described in Section 2.6.

2.12. MALDI-TOF MS and TLC analyses of RfGH5_4 hydrolyzed products from different substrates

Hydrolysis of various cellulosic and hemicellulosic substrates by *Rf*GH5_4 was confirmed by Matrix-Assisted Laser Desorption Ionization – Time-of-Flight Mass Spectrometry (MALDI-TOF MS) and TLC analyses. 100 μL reaction mixture containing 90 μL of 1% (w/v) substrate (barley β-D-glucan, CMC—Na, lichenan, tamarind xyloglucan, HEC, konjac glucomannan, avicel, cellulose powder, PASC, beechwood xylan, birchwood xylan and carob galactomannan) and 10 μL of *Rf*GH5_4 (50 μg/mL) was incubated at pH 5.5 and 30 °C for 2 h. The hydrolysate for each substrate was prepared as discussed in Section 2.11 and the chromatogram was generated.

For mass spectrometric analysis, 1 μL of hydrolysate produced was mixed with 1 μL of DHB (10 mg/mL) matrix (in 50:50%, v/v acetonitrile: water, and 0.1%, v/v trifluoroacetic acid). The analysis was performed as per the earlier reported protocol [24]. MALDI-TOF MS was performed on time-of-flight mass spectrometer Autoflexspeed (Bruker Daltonics, Bremen, Germany) in positive reflectron mode. It was provided with the accelerating voltage of 4.9 × 2400 V. The time delay for pulse ion extraction and laser shot frequency was set at 120 ns and 2000 Hz, respectively. Two thousand shots per sample were recorded. The *m/z* range was plotted from 350 so that interference of high-intensity DHB matrix signals could be minimized.

2.13. Processivity of RfGH5_4

The mode of action of *Rf*GH5_4 was further investigated to get the insights of whether the enzyme was hydrolyzing the cellulosic substrates in a processive (consistent release of two short oligosaccharides) or non-processive manner (random release of higher oligosaccharides). The (100 μL) reaction mixture containing 1% (w/v) PASC (10 mg/mL) in 20 mM citrate-phosphate buffer, pH 5.5 and 10 μL of 50 μg/mL *Rf*GH5_4 was incubated at 30 °C for different time intervals namely, 1, 2, 5, 10, 15, 30 min and 1, 4, 12, and 24 h. By prospecting the role of *Rf*GH5_4 in SSF, 30 °C temperature was selected for the reaction. The Processivity index (PI) (reducing sugar in soluble fraction/reducing ends in insoluble fractions) was calculated by estimating the total reducing sugar in soluble fraction and reducing ends in insoluble fractions as discussed in the Section 2.6. The TLC analysis was performed as described in Section 2.11. The oligosaccharide products generated during hydrolysis of PASC were also analysed by HPLC wherein MetaCarb 67C analytical reverse phase column (300 × 6.5 mm) at 85 °C with double distilled water at 0.5 mL/min flow rate as the mobile phase was used. The chromatogram generated for each reaction was analysed for presence of oligosaccharides using Lab Solution software (Shimadzu, Japan) and was compared with the chromatogram of cellooligosaccharide (G1, G2, G3 and G4) standards generated using the same experimental conditions.

2.14. Deconstruction of lignocellulosic biomass by RfGH5_4

The role of *Rf*GH5_4 in deconstruction of various pre-treated lignocellulosic biomass was explored. The lignocellulosic biomasses (5%, *w/v*) namely, Cotton (*Gossypium hirsutum* L.) Main Stalk (CMS), Cotton Small Branches (CSB), Sugarcane Bagasse (*Saccharum officinarum*) (SBG) *Sorghum Durra* stalk (*Sorghum durra*) (SDR), Finger Millet Stalk (*Eleusine coracana*) (FMS) and Maize Leaves (*Zea mays*) (MZL) were used. The biomasses (5%, *w/v*) were pre-treated by using previously optimized methods, 2% (w/v) NaOH (for CMS and CSB, [25] or 1% (w/v) NaOH (for SBG, [26]; for SDR, [27]; for FMS, [28] and for MZL, [29]) pre-treatment followed by autoclaving at 121 °C for 20 min under 15 psi pressure. The pre-treated biomass was then filtered, neutralised at pH 7.0 using water and dried at 70 °C for 12 h.

For saccharification, each dried pre-treated biomass (2%, w/v) was individually suspended in 600 μL of 20 mM citrate-phosphate buffer, pH 5.5. 10 μL of sodium azide (0.05%, w/v) was also added in the reaction to prevent any contamination. The pre-treated biomasses were independently saccharified in a final reaction volume of 1 mL at 30 °C and 180 rpm for 48 h by using 390 μL of protein from 50 μg/mL stock of purified *Rf*GH5_4 endoglucanase. The final reaction concentration of the *Rf*GH5_4 was 19.5 μg/mL or 87 PASC U/g of biomass. The TRS was estimated as described in Section 2.6, whereas the TLC analysis of hydrolysed products of various biomasses was performed as discussed in Section 2.11.

3. Results and discussion

3.1. Molecular architecture, cloning, expression and purification of RfGH5_4

3.1.1. Molecular architecture of $RfGH5_{1/2}$

The complete genome sequence analysis of *R. flavefaciens* FD-1 v3 reported 14 glycoside hydrolases of family GH5 [30]. *Rf*GH5_4 is a part of the modular enzyme complex, *Rf*$GH5_{1/2}$ from *R. flavefaciens* FD-1 v3 (Fig. 1 a). *Rf*GH5_4 is located at the N-terminal of *Rf*$GH5_{1/2}$ (34–384 amino acids) after a signal peptide (1–27 amino acids) and unknown sequence (28–33 amino acids), while the C-terminal contains an *endo*-mannanase (*Rf*GH5_7, 527–834 amino acids) [13,15]. The two catalytic modules are separated by the family 80 carbohydrate binding module (*Rf*CBM80, 407–502 amino acids). The C-terminal of *Rf*$GH5_{1/2}$ ends with a type I dockerin domain (865–947 amino acids) attached with *Rf*GH5_7 through a linker sequence (835–864 amino acids). *Rf*GH5_4 is listed in the CAZy database as a part of *Rf*$GH5_{1/2}$ (GenBank Accession No. WP_009984467.1). In this study, the gene encoding a putative endoglucanase, *Rf*GH5_4 was cloned, expressed and characterized.

3.1.2. Cloning, expression and purification of RfGH5_4

The gene (1053 bp) encoding the catalytic module, *Rf*GH5_4 without signal peptide and linker sequences was cloned in the pHTP expression vector. It was expressed by using *E. coli* BL21 (DE3) cells followed by the purification using IMAC. The purified protein showed a single, homogenous band of molecular size approximately, 41 kDa as analysed on 12% (w/v) gel by SDS-PAGE analysis (Fig. 1 b, Lane 7). This was found in agreement with the theoretically calculated molecular mass of 41.18 kDa from its amino acid sequence. The purified *Rf*GH5_4 was used for biochemical characterization.

3.2. Biochemical characterization of RfGH5_4

3.2.1. Substrate specificity of RfGH5_4

Various polysaccharides hydrolyzed by *Rf*GH5_4 are listed in Table 1. The maximum enzyme activity exhibited by *Rf*GH5_4 was observed against a β-1,3; 1,4 mixed polysaccharide barley β-D-glucan (665 U/mg). Efficient hydrolysis of CMC-Na (450 U/mg), lichenan (393 U/mg), xyloglucan (343 U/mg), HEC (333 U/mg) and konjac

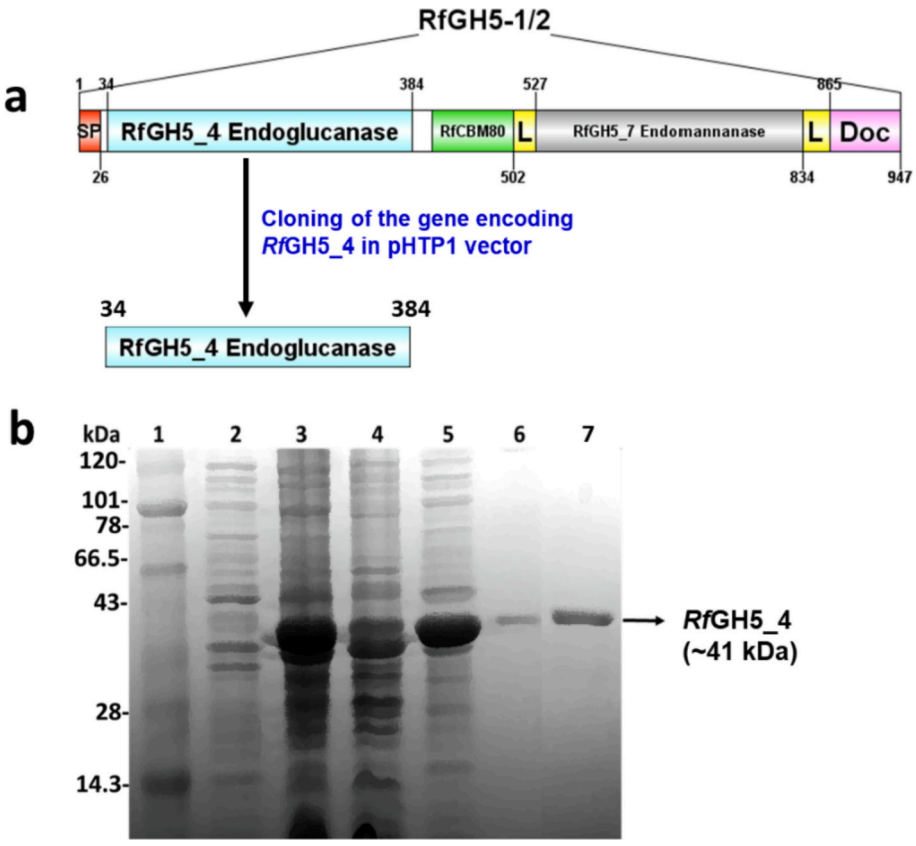

Fig. 1. Molecular architecture of (a) *Rf*GH5$_{1/2}$ protein complex containing *Rf*GH5_4 was constructed by Dog 2.0 software. It shows the signal peptide (SP) at N-terminal followed by an endoglucanase module *Rf*GH5_4, family 80 carbohydrate binding module (CBM80) and endomannanase catalytic module, *Rf*GH5_7. L represents linker, while D is a type I dockerin domain present at C-terminal. SDS-PAGE analysis (b) of *Rf*GH5_4 purification steps on 12% (*w/v*) gel. Lanes, 1- protein mass marker (BioBharti, India), 2 - Un-Induced *E. coli* BL21 (DE3) cells, 3: Induced *E. coli* BL21 (DE3) cells at 1 mM IPTG, 4 - Induced Cell Pellet (after sonication), 5 - Cell-Free Extract, 6 - Last Column Wash, 7 - showing band of purified protein *Rf*GH5_4 (*Approx*. 41 kDa).

Table 1
Substrate specificity of *Rf*GH5_4 from *R. flavefaciens* FD-1 v3.

Substrate (1.0%, w/v)	Specific activity (U/mg)
Barley β-D-glucan	665 ± 8
CMC-Na	450 ± 10
Lichenan	393 ± 8
Hydroxyethyl cellulose (HEC)	333 ± 3
Phosphoric Acid Swollen Cellulose (PASC)	86.6 ± 2.6
Cellulose powder	0.32 ± 0.02
Avicel	0.21 ± 0.01
Tamarind xyloglucan	343 ± 1
Konjac glucomannan	285 ± 12
Carob galactomannan	16 ± 1
Beechwood xylan	21.7 ± 4.5
Birchwood xylan	9.7 ± 3.3

All the experiments were carried in triplicates ($n = 3$) and mean ± SD for each experiment is shown here.

glucomannan (285 U/mg) by *Rf*GH5_4 was also observed. Interestingly, *Rf*GH5_4 was able to hydrolyze PASC (86.6 U/mg), cellulose powder (0.3 U/mg) and microcrystalline avicel (0.2 U/mg). Similar results were obtained for endoglucanases from *Clostridium cellulovorans* where multifunctional endoglucanases, *EngB* and *EngD* hydrolyzed pure micro granular cellulose (51 and 37 U/mg, respectively) and microcrystalline avicel (20 and 16 U/mg, respectively) at pH 6.0 and 37 °C temperature in a 12 h incubation assay [31]. *EngB* and *EngD* enzymes also hydrolyzed CMC (82 and 86 U/mg, respectively) along with lichenan (853 and 555 U/mg, respectively). However, an endoglucanase from *R. flavefaciens* FD-1 showed activity against CMC—Na, but no hydrolysis of avicel was observed [32]. Similarly, the endoglucanase from *Bacillus pumilus* hydrolyzed only CMC—Na, but could not act upon avicel [33]. Surprisingly, *Rf*GH5_4 hydrolyzed hemicellulosic substrates with significant activities such as beechwood xylan (21.7 U/mg), birchwood xylan (9.7 U/mg) and carob galactomannan (16 U/mg), displaying its broad substrate specificity. However, the hydrolysis of above mentioned hemicellulosic substrates by *Rf*GH5_4 was significantly lower when compared with the cellulosic substrates (Table 1).

The multifunctionality is less commonly observed among endoglucanases. This characteristic of *Rf*GH5_4 is noteworthy here, which hydrolyses cellulosic as well as hemicellulosic substrates with a notably higher or significant activity. As indicated in a recent report, aromatic residues like tryptophan near the active site protruding outwards from the surface of the protein could be credited for the substrate selectivity and multifunctionality of GH5_4 glucanases [34]. The efficient hydrolysis of cellulosic substrates like CMC-Na and PASC and various hemicellulosic polymers such as barley β-D-glucan and lichenan by *Rf*GH5_4 makes it a potential cellulase candidate in the valorisation of lignocellulosic biomass. Overall, the multifunctional nature of *Rf*GH5_4 widens its canvas in the application sectors like bioenergy, synthesis of prebiotics, modification of cellulosic surfaces, paper, pulp, food and pharmaceutical industry [35].

3.2.2. Biochemical properties of RfGH5_4

The optimization of pH and temperature for the assay of *Rf*GH5_4 was performed by using CMC-Na as the substrate. Maximum activity of *Rf*GH5_4 was recorded at the temperature of 55 °C and pH 5.5 (Fig. 2 a and b, respectively). *Rf*GH5_4 retained most of its activity in the temperature range of 5 °C–45 °C for 1 h of incubation (Fig. 2 c). It retained 75% activity at 45 °C after 1 h of incubation. However, the enzyme was less stable at its optimum reaction temperature of 55 °C, at which the enzyme was almost inactive after 1 h of incubation. *Rf*GH5_4 displayed stability in the pH range, 5–8 of 20 mM sodium phosphate and MES buffers (Fig. 2 d). Thus, despite being optimally active at higher temperature, *Rf*GH5_4 would be most suitable for cellulosic bioethanol production at the temperature of 30 °C displaying significant activity of 149 U/mg. Moreover, 30 °C being an appropriate temperature for fermentation purposes, *Rf*GH5_4 could help in single-step fermentation

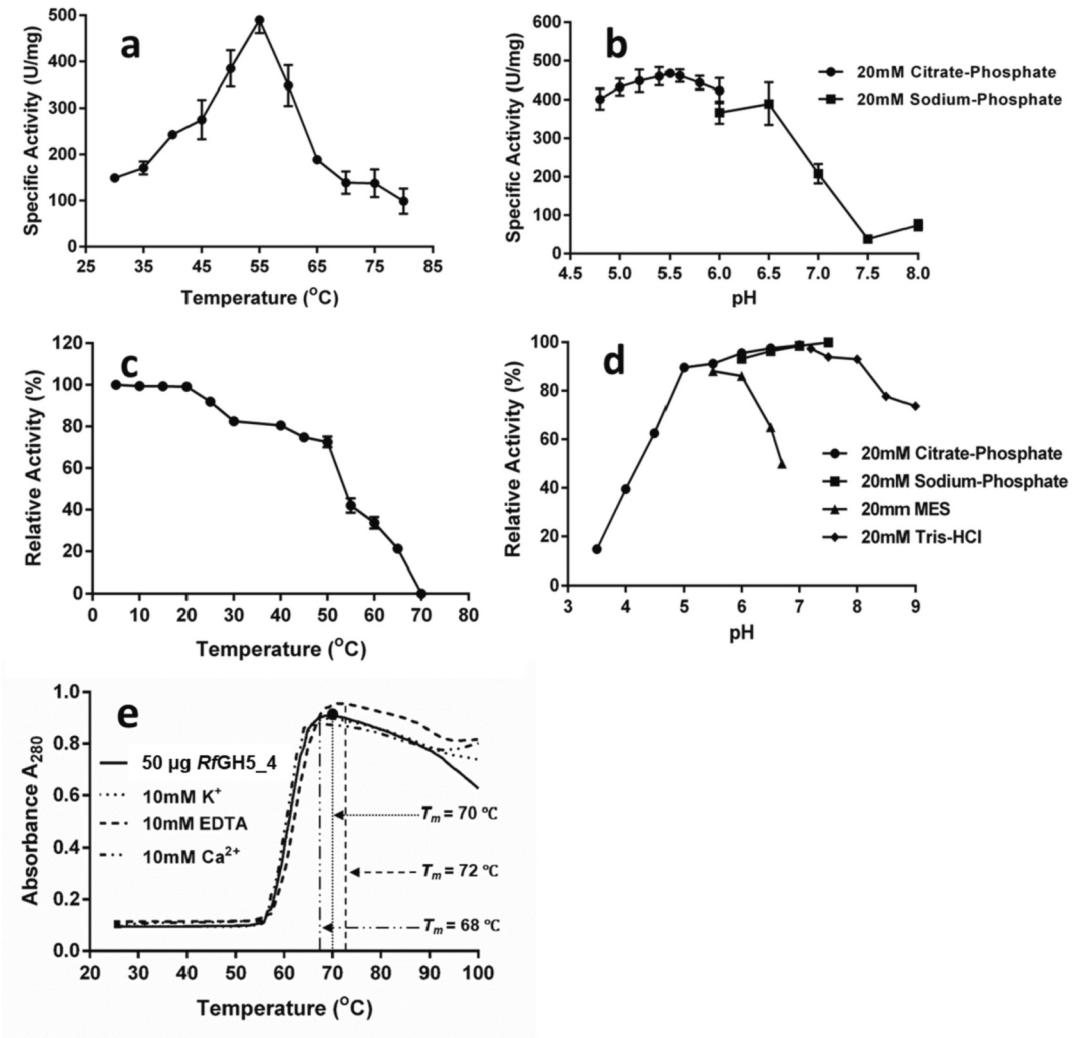

Fig. 2. Optimum reaction (a) temperature, (b) optimum pH, (c) thermostability and (d) pH-stability of *Rf*GH5_4 is shown. All experiments were carried out in triplicates. The data shown here are the mean of three independent experiments. Error bars indicate standard deviation (±SD) for each data point. Melting curve analysis (e) of *Rf*GH5_4 was performed in which 50 µg/mL of *Rf*GH5_4 was incubated independently as well as with 10 mM of EDTA, K^+, or Ca^{2+} ions in 20 mM MES buffer (pH 5.5). The reaction mixture was subjected to varying range of temperatures (25 °C – 100 °C). The absorbance (A_{280}) was recorded at 280 nm.

such as SSF. The ethanol tolerance analysis of *Rf*GH5–4 at 30 °C for 96 h showed that *Rf*GH5_4 is able to tolerate around 20% of ethanol, where it could retain 80% of its activity (Fig. S1). The highest concentration of ethanol achieved during SSF reported is around 7% [36]. Whereas, *Rf*GH5_4 retained 95% activity at 7% ethanol after 96 h of incubation. Thus, the higher ethanol tolerance of *Rf*GH5_4 enhances its suitability for SSF.

3.2.3. *Effect of metal ions and other additives on RfGH5_4 activity*

The influence of various cations and additives on the activity of *Rf*GH5_4 was explored using CMC-Na as the substrate. The activity of *Rf*GH5_4 increased in the presence of 10 mM of K^+ or Li^+ ions (Table 2). A family GH5 endoglucanase, *CelRH5* from the rhizosphere, also showed a similar type of increase in enzyme activity in the presence of Li^+ or K^+ ions [10]. K^+ and Li^+ cations can alter the active site structure of endoglucanase, thereby increasing the enzyme activity [37]. The K^+ ions may be performing the role of mediator between the substrate and the enzyme active site, the characteristic of Type II enzyme activator thereby making conformational changes in *Rf*GH5_4 as also reported earlier [38]. Thus, the increment in the enzyme activity of *Rf*GH5_4 in presence of K^+ ions could be due to their participation at the active site, thereby stabilizing the intermolecular interactions. The use of K^+ ions during synergistic saccharification of lignocellulosic biomasses to enhance the enzyme activity of *Rf*GH5_4 could be further explored. 10 mM of the Mg^{2+} and Na^+ ions decreased the enzyme activity of *Rf*GH5_4 by 33% and 8%, respectively. Surprisingly, Ca^{2+} ions at 10 mM concentration drastically lowered the *Rf*GH5_4 enzyme activity to 29%. Similarly, Ni^{2+}, Fe^{2+}, Co^{2+}, Zn^{2+}, Mn^{2+} and Cu^{2+} ions adversely affected the enzyme activity of *Rf*GH5_4, where 80% to 100% loss in the enzyme activity of *Rf*GH5_4 was observed (Table 2). A similar abrupt decrease in the enzyme activity by these metal ions was also reported for endoglucanase, *Ba-EGA* from *Bacillus* sp. AC-1 [39] and *CelRH5* from rhizosphere [10].

Interestingly, *Rf*GH5_4 enzyme activity was increased by 10% in the presence of 10 mM of EDTA. Similarly, 10 mM of EGTA displayed an increment of 32% in the enzyme activity of *Rf*GH5_4 (Table 2). The increase in the enzyme activity by EDTA and EGTA indicated the absence of Ca^{2+} or Mg^{2+} ions in the *Rf*GH5_4 structure [40]. This increment in the enzyme activity could be attributed to a flexible conformational change, increased k_{cat} and overall stability of *Rf*GH5_4 imparted by these chelating agents as reported for an endoglucanase from fungus, *Aspergillus aculeatus*. 10 mM guanidine hydrochloride drastically decreased the *Rf*GH5_4 enzyme activity by 23%, whereas it was reduced by 15% (w/v) in the presence of 100 mM urea. *Rf*GH5_4 retained 98% and 99% of enzyme activity in presence of 1% (v/v) DMSO and 10% (v/v) glycerol, respectively. The enzyme activity of *Rf*GH5_4

Table 2
Effect of metal ions and additives on *Rf*GH5_4 enzyme activity.

Metal ion (10 mM)/additive	Relative enzyme activity (%)
Control	100 ± 9
Mg^{2+}	67.2 ± 3.7
Ca^{2+}	29 ± 4
Na^{+}	92.4 ± 4.5
K^{+}	150 ± 2
Mn^{2+}	0.9 ± 0.6
Li^{+}	106.1 ± 2.8
Co^{2+}	13.5 ± 5.9
Ni^{2+}	14.1 ± 2.4
Fe^{2+}	0
Zn^{2+}	0
Cu^{2+}	0
EDTA (10 mM)	110.2 ± 2.9
EGTA (10 mM)	132.4 ± 2.2
Guanidine hydrochloride	77 ± 3
Urea (100 mM)	85 ± 5
DMSO (1%, v/v)	98 ± 3
Glycerol (10%, v/v)	99 ± 6
Triton X-100 (0.5%, v/v)	108.7 ± 8.7
Tween 80 (1%, v/v)	83 ± 11
SDS (0.1%, w/v)	0

All the experiments were carried in triplicates ($n = 3$) and mean ± SD for each experiment is shown here. Specific activity of Control was 341 U/mg and was considered as 100%.

was increased in presence of 0.5% (v/v) Triton X-100 by 8.7%, whereas 1% (v/v) Tween 80 decreased the activity of *Rf*GH5_4 by 17% (Table 2). *Rf*GH5_4 lost 100% of enzyme activity in the presence of 0.1% SDS which remarks the sensitivity of *Rf*GH5_4 towards anionic detergents. Endoglucanase *CS10* from *Hermetia illucens* was reported with a similar type of decrease in the enzyme activity in the presence of guanidine hydrochloride, urea and SDS [41].

3.3. Protein melting analysis of RfGH5_4

The complete melting of *Rf*GH5_4 was observed at 70 °C (T_m). The addition of 10 mM EDTA slightly increased the T_m of *Rf*GH5_4 by 2 °C (72 °C), showing the absence of any metal ion in the enzyme structure (Fig. 2 e). This result corroborated with the result from the previous section, where incubation of *Rf*GH5_4 with 10 mM EDTA increased the enzyme activity by 10%, indicating the absence of any metal ion in the structure. A decrease in the T_m of *Rf*GH5_4 by 2 °C was observed by 10 mM of Ca^{2+}. This was also in agreement with results of previous section, where 10 mM of Ca^{2+} ions lowered to 29% of the enzyme activity, thereby displaying the role of Ca^{2+} ions in destabilizing the *Rf*GH5_4 structure. 10 mM of K^{+} ions did not affect the T_m of *Rf*GH5_4 (70 °C). However, K^{+} ions displayed increase in the enzyme activity of *Rf*GH5_4 as mentioned in the previous section. It is possible that the K^{+} cations play a role in the catalysis of *Rf*GH5_4 affecting its conformation rather than its stability as observed for an endoglucanase from a plant root ericoid mycorrhizal fungus *Leohumicola* sp. [37,42].

3.4. Kinetic parameters of RfGH5_4

The kinetic parameters of endoglucanase, *Rf*GH5_4 against various carbohydrate substrates were determined and are summarized in Table 3. *Rf*GH5_4 showed remarkably high V_{max} and low K_m against different substrates (Fig. 3 a, b, c and d). It displayed a turnover number (k_{cat}, sec^{-1}) of 473 and 360.3 for β-D-glucan and CMC—Na, respectively. The V_{max} of 525 U/mg by *Rf*GH5_4 against CMC-Na was significantly higher than V_{max}, 160.6 U/mg reported for endoglucanase *CS10* cloned from the gut microflora of the black soldier fly, *Hermetia illucens* [41]. The catalytic efficiency (k_{cat}/K_m) and K_m of *Rf*GH5_4 for CMC-Na was deduced to be 146 $mL.mg^{-1}\ s^{-1}$ and 2.47 mg/mL, respectively (Table 3).

Recently, a multifunctional glucomannanase, *6XSU* of subfamily

Table 3
Kinetic properties of *Rf*GH5_4.

Substrate[a]	V_{max} (U/mg)	K_m (mg/mL)	k_{cat} (s^{-1})	k_{cat}/K_m ($mL.mg^{-1}\ s^{-1}$)
β-D-glucan	689 ± 18	0.54 ± 0.04	473 ± 18	875.7 ± 33.9
Lichenan	495 ± 9	0.58 ± 0.05	339.7 ± 7.4	585.7 ± 12.8
CMC-Na	525 ± 14	2.47 ± 0.14	360.3 ± 11.7	146 ± 5
Hydroxyethyl Cellulose (HEC)	371 ± 27	1.43 ± 0.30	254.6 ± 23.9	178 ± 16
Tamarind Xyloglucan	381 ± 12	0.89 ± 0.01	261.4 ± 10.1	294 ± 11
Konjac Glucomannan	316 ± 5	0.41 ± 0.02	216.8 ± 5.2	529 ± 12

[a] The assays were carried out in triplicates (n = 3) with 5 μg/mL (final concentration) of RfGH5_4 at an optimum pH 5.5 (20 mM citrate phosphate buffer) and 55 °C for 2 min. Mean ± SD for each experiment is shown here.

GH5_4 from *R. flavefaciens* was reported with the K_{cat}/K_m ($mL.mg^{-1}\ s^{-1}$) of 5.66 for glucomannan and 1.55 for xyloglucan at 30 °C [34]. These values are significantly lower to those of *Rf*GH5_4 against these two substrates, 529 and 294, respectively, at 55 °C. This large difference in k_{cat}/K_m values of *Rf*GH5_4 and *6XSU* could be due to the difference in the reaction temperature used for determination of kinetic parameters. In the present state, fungal cellulases dominate the industrial cellulase market. The most studied and industrially used organism for cellulase production, *Trichoderma reesei*, displays the catalytic efficiency of 7.3 $mL.mg^{-1}\ s^{-1}$ and K_m of 5 mg/mL (at pH 5.0, 30 °C) for its endoglucanase, *EGIII (Cel12A)* against CMC-Na [43]. *EGIII* displays the highest catalytic efficiency among all the *T. reesei* endoglucanases. An attempt to increase the catalytic efficiency of *EGIII* resulted in a *2R4* mutant giving enhanced pH and thermostability but with a decrease in the catalytic efficiency to 4.8 $mL.mg^{-1}\ s^{-1}$ [44].

The phylogenetic analysis of *Rf*GH5_4 and fungal endoglucanases of CAZy GH5 family showed that *Rf*GH5_4 shares the nearest evolutionary relationship with GH5 fungal endoglucanases *Epi2* (*Epidinium caudatum*), *CelA* (*Neocallimastix frontalis*) and *CelD* (*Neocallimastix patriciarum)* (Fig. S2). The multiple sequence alignment of *Rf*GH5_4 with GH5 fungal endoglucanases was also performed (Fig. S3) which revealed that the catalytic residues of *Rf*GH5_4 (E168 and E292) have survived the evolution and are also conserved in all the GH5 fungal endoglucanases including the popular *EGII (Cel5A)* (formerly, *EGIII-Cel5A*) of *Trichoderma reesei*. Other conserved residues are H122 and W325. Singh et al. [1] reported 32.1 U/mg specific activity of an Ultra Violet (UV) radiated CMCase mutant, CMCase-UV2 from *Bacillus amyloliquefaciens* SS35 which is significantly lesser than 525 U/mg activity of *Rf*GH5_4 against CMC-Na (Table 3). Another endoglucanase, *CtCel5E* (GH5) from *Clostridium thermocellum*, had specific activity of 736.2 U/mg against CMC-Na [45]. However, k_{cat}/K_m of 12.40 $mL.mg^{-1}\ s^{-1}$ and K_m of 2.1 mg/mL of *CtCel5E* against CMC-Na (pH 5.0, 50 °C) is remarkably lower than 146 $mL.mg^{-1}\ s^{-1}$ of *Rf*GH5_4 (Table 4). A processive endoglucanase, EG5C [46] and EG5C-1 D70Q/S235W [47] from *Bacillus subtilis* BS-5 showed k_{cat}/K_m of 38 and 37.3 $mL.mg^{-1}\ s^{-1}$, respectively against CMC-Na as the substrate.

It could be concluded that k_{cat}/K_m of *Rf*GH5_4 is much higher than those of *EG III* and *CtCel5E*. Moreover, K_m of *Rf*GH5_4 against CMC-Na is relatively, lower than those *EGIII* and *CtCel5E* (Table 4).

*Rf*GH5_4 hydrolyzed tamarind xyloglucan with a significantly high specific activity (V_{max}, 381 U/mg) at relatively low substrate concentration (K_m, 0.89 mg/mL). An endoglucanase, *XEG5* of *Paenibacillus* sp. *XEG5* showed the V_{max} of 18.4 U/mg against tamarind xyloglucan, which is notably lower than that of *Rf*GH5_4 [51]. Moreover, the appreciable catalytic efficiency of *Rf*GH5_4 over a wide range of cellulosic and hemicellulosic substrates is noteworthy (Table 3). The kinetic

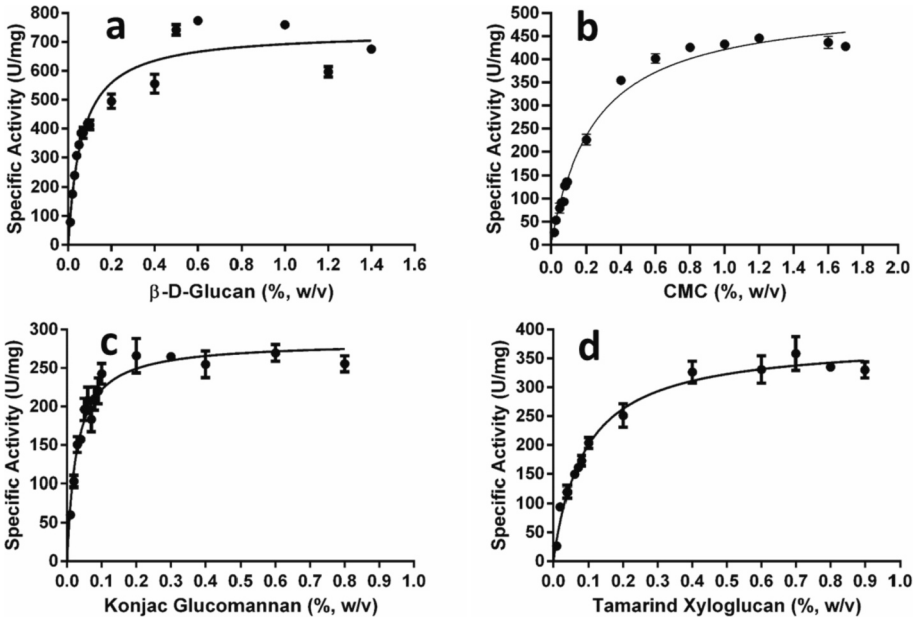

Fig. 3. Michaelis-Menten kinetics of *Rf*GH5_4 against (a) barley β-D-glucan, (b) CMC—Na, (c) konjac glucomannan and (d) tamarind xyloglucan was studied at optimum pH of 5.5 and 55 °C temperature (in 20 mM citrate-phosphate buffer) at final enzyme concentration of 5 μg/mL. The inset of every diagram shows the Lineweaver-Burk plot of *Rf*GH5_4 against respective substrates. All experiments were carried out in triplicates. The data shown here are the mean of three independent experiments. Error bars indicate standard deviation (±SD) for each data point.

Table 4
Comparison of some currently known and commercial endoglucanases with *Rf*GH5_4.

Enzyme	Substrate	Organism	Optimum	Kinetics	Reference
Endoglucanase, *Rf*GH5_4	CMC-Na	*Ruminococcus flavefaciens* FD-1 v3	pH 5.5, 55.5 °C, 41.18 kDa	*SA* – 450 K_m – 2.47 k_{cat}/K_m – 145.9	This study
Endoglucanase, *Egst*	CMC-Na, Medium Viscosity	*Scytalidium thermophilum*	pH 5.5, 60 °C, 66 kDa	*SA* – 246 K_m – 10.5 k_{cat}/K_m – 45.2	[48]
β-1,4-endoglucanase, *rMt-egl*	CMC-Na	*Myceliopthora thermophila BJA*	pH 10, 50 °C, 47 kDa	*SA* – 119.4 K_m – 5 k_{cat}/K_m – 204	[49]
Bifunctional Cellulase, *CtCel5E,* (GH5)	CMC	*Clostridium thermocellum*	pH 5.0, 50 °C	*SA* – 736 K_m – 2.1 k_{cat}/K_m – 12.40	[45]
β-1,4-endoglucanase, *TaEGII*	CMC-Na	*Trichoderma atroviride*	pH 5.0, 60 °C, 44.23 kDa	*SA* – 119.4 K_m – 0.014 k_{cat}/K_m – 6.50	[50]
Endoglucanase, *EGIII (Cel12A)*	CMC-Na	*Trichoderma reesei*	pH 5.0, 30 °C, *48 kDa*	*SA* – 351 K_m – 5 k_{cat}/K_m – 7.33	[43]
Spezyme#3 (β-1,4-endoglucanase)	CMC-Na	*Trichoderma reesei*	pH 4.0, 50 °C	*SA* – 25	Genencor Intl., USA
Cellulase AP30K (β-1,4-endoglucanase)	CMC-Na	*Trichoderma reesei*	pH 4.5, 60 °C	*SA* – 21	Amano Enzyme, USA
*E-CELTH (*β-1,4-endoglucanase, GH6)	CMC-Na	*Thermobifida halotolerans*	pH 8.5, 80 °C	*SA* – 16	Megazyme Ltd., Ireland
ACCELLERASE 1500 (β-1,4 endoglucanase)	CMC-Na	*Trichoderma reesei*	pH 4.8, 50 °C	*SA* – 2.8	DuPont De Nemours, Inc. USA
C2730-Celluclast (β-1,4-endoglucanase)	Bacterial Cellulose, Paper grid	*Trichoderma reesei*	pH 6, 52 °C	*SA* – 0.7	Sigma-Aldrich Corp. / Novozyme Corp., USA
C1184-Cellulase (β-1,4-endoglucanase)	Cellulose	*Aspergillus niger*	pH 5, 37 °C	*SA* – 0.3	Sigma-Aldrich Corp. / Novozyme Corp., USA

SA = Specific Activity (U/mg), K_m = mg/mL, k_{cat}/K_m = mL.mg^{-1} s^{-1}.

parameters and the catalytic efficiencies of some recently studied (including this study) and commercially available endoglucanases are described in Table 4. *Rf*GH5_4 stands out as an efficient multifunctional endoglucanase among the other known endoglucanases. The comparison underlines the potential of *Rf*GH5_4 for industrial applications like lignocellulosic bioethanol production over the other available endoglucanases.

3.5. Hydrolysis mechanism and multifunctionality of RfGH5_4

3.5.1. Hydrolytic mechanism analysis of RfGH5_4 using TLC

A chromatogram developed with the CMC-Na hydrolysates produced by *Rf*GH5_4 displayed cellotriose, cellotetraose and other higher oligosaccharides after 2 min of reaction in a 24 h hydrolysis (Fig. 4 a). However, after 1 h, cellotriose was a predominant oligosaccharide along with other higher oligosaccharides (>DP4), confirming the *endo*-acting catalytic mode of *Rf*GH5_4. Quantification of reducing sugars revealed

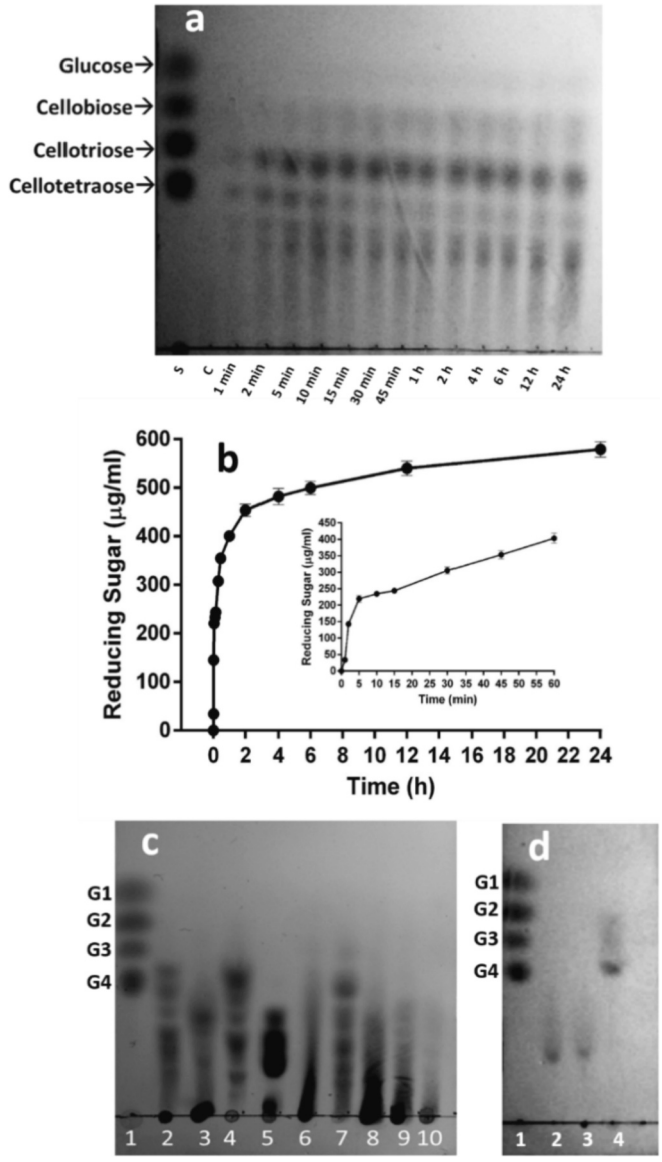

Fig. 4. Time-dependant TLC analysis of hydrolyzed products of CMC-Na by *Rf*GH5_4 was carried out. (a) Chromatogram of TLC of the hydrolysate of CMC-Na by *Rf*GH5_4 for different time intervals. Lane S represent Standards (Glucose, Cellobiose, Cellotriose, Cellotetraose) and lane 2 is Control (C) without enzyme. Other lanes are time-dependent enzyme reaction products of *Rf*GH5_4 with CMC—Na. (b) Plot of reducing sugar concentration with time. Inset shows the reducing sugar released in the first 60 min. The assay was performed with the 50 µg/mL final enzyme concentration of *Rf*GH5_4 at 30 °C and pH 5.5 (20 mM citrate-phosphate) for 1 min to 24 h. The TLC analysis of *Rf*GH5_4 generated hydrolysates (c) of different carbohydrate polymers was also performed. Lanes, 1- Standards: G1-glucose, G2-cellobiose, G3-cellotriose and G4-cellotetraose. 2- barley β-D-glucan, 3- CMC—Na, 4- lichenan, 5- tamarind xyloglucan, 6- HEC, 7- konjac glucomannan, 8- beechwood xylan, 9- birchwood xylan, 10- carob galactomannan. Hydrolysates of avicel, cellulose powder and PASC are shown in Fig. (d). Lanes, 1- Standards: G1- glucose, G2- cellobiose, G3- cellotriose and G4- cellotetraose, 2- avicel, 3-cellulose powder, 4- PASC. The assay was performed with 50 µg/mL working concentration of *Rf*GH5_4 at 30 °C in 20 mM citrate-phosphate, pH 5.5 and. For avicel, cellulose powder and PASC, a rotation of 200 rpm was provided for 2 h.

that the hydrolysis process achieved saturation after 12 h of the reaction (Fig. 4 b).

3.5.2. TLC and MALDI-TOF MS of *RfGH5_4* hydrolyzed products from different substrates

The hydrolysis of various substrates by *Rf*GH5_4 was analysed and confirmed by TLC. The substrates used were barley β-D-glucan, CMC—Na, lichenan, tamarind xyloglucan, HEC, konjac glucomannan, beechwood xylan, birchwood xylan and carob galactomannan. Moreover, the release of various degrees of oligosaccharides by *Rf*GH5_4 was observed. Cellobiose, cellotriose, cellotetraose and other higher cellooligosaccharides could be detected in the barley β-D-glucan, CMC-Na and HEC hydrolysates (Fig. 4 c, Lanes 2, 3 and 6, respectively). Cellotetraose was the primary product in lichenan and konjac glucomannan hydrolysis (Fig. 4 c, Lanes 4 and 7, respectively). The hydrolysis of xyloglucan showed multiple spots on the TLC plate which were attributed to different xyloglucan oligosaccharides (XyGs), as confirmed by MALDI-TOF MS analysis (Fig. 4 c, Lane 5). The TLC analysis also confirmed the hydrolysis of beechwood xylan, birchwood xylan and carob galactomannan by *Rf*GH5_4 (Fig. 4 c, Lanes 8, 9 and 10, respectively) for which released oligosaccharides (DP2 to DP11) were also recognized with the help of MALDI-TOF MS analysis. The cellooligosaccharides higher than cellotetraose were observed in the hydrolysates of avicel and cellulose powder (Fig. 4 d, Lane 2 and 3, respectively). However, PASC was hydrolysed to oligosaccharides smaller than cellotetraose like cellotriose and cellobiose (Fig. 4 d, Lane 4). The crystallinity index (*CrI*) of PASC was recorded to be 0 to 0.04 which makes the cellulose chains freely accessible to the endoglucanase, unlike avicel, for which the *CrI* ranges between 0.5 and 0.6 [52]. Higher the *CrI* of a cellulosic substrate, lower is the accessibility of an endoglucanase for the cellulose chain and vice-versa.

The MALDI-TOF MS (DP, *m/z* ratio) analysis revealed that *Rf*GH5_4 randomly hydrolyses β-D-glucan to give cellooligosaccharides ranging from DP2 to DP12, thus further confirming *Rf*GH5_4 as an endoglucanase (Fig. S4 a). Lichenan hydrolysate of *Rf*GH5_4 also contained cellooligosaccharides in the range of DP2-DP12 (data not shown). MALDI-TOF analysis of PASC hydrolysate revealed the presence of majorly cellobiose (DP2) and cellotriose (DP3) (Fig. S4 b), indicating the processive hydrolysis of amorphous cellulose by *Rf*GH5_4 as also described and confirmed in the Section 3.6. CMC-Na hydrolysate of *Rf*GH5_4 showed cellooligosaccharides ranging between DP2 and DP6 (data not shown). Only higher cellooligosaccharides of size DP8 to DP10 were detected in the hydrolysates of avicel and cellulose powder by MALDI-TOF MS analysis (data not shown), thus confirming complex cellulose hydrolysis by *Rf*GH5_4. Glucose was not detected in any of these hydrolysates upon the MALDI-TOF analysis.

Hydrolysate of konjac glucomannan from *Rf*GH5_4 (Fig. S4 c) showed oligosaccharides of DP2 (*m/z* ratio, 365), DP3 (527), DP4 (689), DP5 (851.2), DP6 (1013.2) and DP7 (1175.2) thus revealing the glucomannanase function of *Rf*GH5_4. The presence of oligosaccharides ranging from DP3 to DP7 in the hydrolysate of *Rf*GH5 treated carob galactomannan as analysed by MALDI-TOF MS, confirmed its activity on the main chain of galactomannan randomly cleaving the β-1,4 linked mannose units thus revealing it as an endomannanase (Fig. S4 d). Xyloglucan oligosaccharides obtained after hydrolysis of tamarind xyloglucan by *Rf*GH5_4 were, XXXG (1085.9), XLXG (1248), XXLG (1248) and XLLG (1410.2) showing it to be a xyloglucanase (Fig. S4 e). Subfamily 4 endoglucanases from family GH5 uniquely hydrolyse xyloglucan as can be also observed for *Rf*GH5_4. Moreover, *Rf*GH5_4 multifunctional endoglucanase could also be the member of EC 3.2.1.151 along with being a member of EC 3.2.1.4, because it also efficiently hydrolyses β-(1,4) main chain linkage of xyloglucan. Xyloglucan specific endoglucanase from *Paenibacillus* sp. strain KM21 was reported in EC 3.2.1.151 family [6]. *Rf*GH5_4 also hydrolysed beechwood xylan (Fig. S4 f) and birchwood xylan (data not shown) as can be stated from the presence of xylooligosaccharides ranging from DP2 to

DP12 in their respective hydrolysates. Thus, the MALDI-TOF MS analyses of different substrate hydrolysates confirmed the multi-functionality and broad substrate specificity of *Rf*GH5_4. Various degrees of oligosaccharides detected in the hydrolysates of *Rf*GH5_4 treated substrates further confirmed its *endo*-acting mode of polysaccharide hydrolysis.

3.6. Processivity of RfGH5_4 on cellulose

The mode of cellulose hydrolysis by *Rf*GH5_4 was elucidated. The processivity of *Rf*GH5_4 was studied at different time intervals up to 24 h, as shown in the TLC analysis. *Rf*GH5_4 hydrolysed the cellulosic substrate, PASC and gave cellotetraose during first 30 min of the reaction. However, consistent release of cellotriose and cellobiose was observed after 1 h of the reaction (Fig. 5 a). This is the processive behaviour of *Rf*GH5_4 endoglucanase, where it consistently cleaved PASC into cellotriose and cellobiose and this mode is called processivity as reported earlier [53]. The HPLC chromatogram of PASC hydrolysates from different time intervals also showed that the release of cellooligosaccharides from PASC was confined to cellotriose (G3) and cellobiose (G2) after 1 h of the reaction further confirming the processivity of *Rf*GH5_4 (Fig. 5 b). The chromatogram of cellooligosaccharide standards (G1-G4) was generated to recognize the respective oligosaccharides in PASC hydrolysates (Fig. S5). The PI of the hydrolysis reaction of *Rf*GH5_4 on PASC was found consistently increasing from 0.1 to 4.9 (Table 5) in a 1 min to 24 h assay, further confirming the processive behaviour of *Rf*GH5_4.

In the PI analysis, the accumulation of soluble reducing sugars usually increases with time, whereas the reducing ends of cellulose in the insoluble un-hydrolysed substrate fractions remain constant. The processive endoglucanases show an increasing PI over a time period of incubation as also observed for *Rf*GH5_4 (Fig. 5 c). Zheng et al. [53] also reported the initial release of cellotetraose followed by cellotriose and cellobiose from PASC by an GH5 endoglucanase, *EG1* from fungus *Volvariella volvacea*. As observed for *Rf*GH5_4, the processive endoglucanases, EG5C and EG5C-1 from *Bacillus subtilis* also showed the release of cellobiose and cellotriose from PASC and Avicel [46]. Processivity is rarely observed in endoglucanases from family GH5. Therefore, the processive endoglucanases from family GH5 should be explored for their applications in renewable energy sector.

The drawback of using non-processive endoglucanases in biomass conversion is that they produce only higher oligosaccharides unlike *Rf*GH5_4. Therefore, processive endoglucanase, *Rf*GH5_4 can be used for bioethanol production that releases significant amount of cellobiose through its processivity during lignocellulosic biomass conversion.

3.7. Hydrolysis of lignocellulosic biomasses by RfGH5_4

The compatibility of *Rf*GH5_4 endoglucanase for saccharification of lignocellulosic biomass was observed. Six different types of alkali pre-treated biomasses viz. CMS, CSB, SBG, SDR, FMS, MZL were hydrolysed by *Rf*GH5_4 in to various degree of oligosaccharides in the 48 h of saccharification (DP4-DP2 and >DP4) (Fig. 6 a). Highest TRS (mg/g of biomass) was achieved by 87 U/g of *Rf*GH5_4 through the hydrolysis of SDR (72) followed by FMS (62), SBG (38), CSB (27), CMS (19) and MZL (8.5) (Fig. 6 b). The TRS yield generated by *Rf*GH5_4 from alkali pre-treated SDR and SBG was significantly higher than the earlier reported TRS yields for these biomasses (34.2 mg/g for SDR, [27] and 5.9 mg/g for SBG, [54]. Jamaldheen et al. [27] used endoglucanase (*Ct*Cel8A, 80 U/mg) and β-glucosidase (*Ct*Bgl1A, 33 U/mg) of *C. thermocellum* for SDR saccharification. Nath et al. [54] employed chimera, *Ct*GH1-L1-*Ct*GH5-F194A (240 U/g) containing β-glucosidase and endoglucanase along with cellobiohydrolase, *Ct*CBH5A (360 U/g) from *C. thermocellum* to saccharify SBG. However, the TRS yield from *Rf*GH5_4 saccharified CMS and CSB was comparatively lower than the reported value (490 mg/g) in a previous report [25], where the alkali pre-treated 5% (w/v) cotton

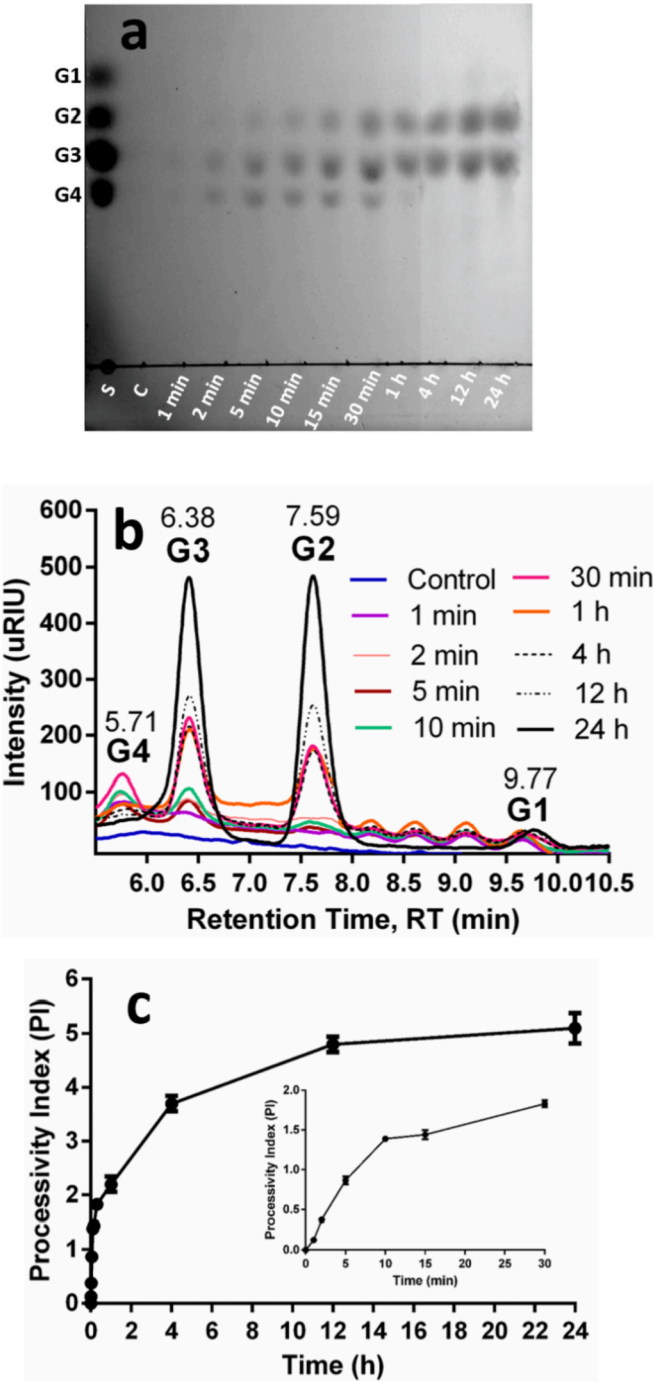

Fig. 5. Time-dependant TLC analysis of hydrolyzed products of PASC by *Rf*GH5_4 was carried out. (a) The Chromatogram shows the TLC of the hydrolysate of PASC by *Rf*GH5_4 for different time intervals. Lane S represent Standards (G1, Glucose, G2, Cellobiose, G3, Cellotriose, G4, Cellotetraose) and lane 2 is Control (C) without enzyme. Other lanes are time-dependent enzyme reaction products of PASC by *Rf*GH5_4. The assay was performed with the 50 μg/ml final enzyme concentration of *Rf*GH5_4 at 30 °C and pH 5.5 (20 mM citrate-phosphate) for 1, 2, 5, 10, 15, 30 min and 1, 2, 4, 12, and 24 h. (b) HPLC analysis of the *Rf*GH5_4 generated time dependent hydrolysates of PASC. (c) Processivity Index (PI) analysis of *Rf*GH5_4 with the time-dependant hydrolysis of PASC was performed with the 50 μg/ml final enzyme concentration of *Rf*GH5_4 at 30 °C and pH 5.5 (20 mM citrate-phosphate) for 1, 2, 5, 10, 15, 30 min and 1, 2, 4, 12, and 24 h. Control without enzyme was also run. The ratio of reducing sugars released by *Rf*GH5_4 in soluble fractions to the reducing ends of insoluble fraction (PI) was then determined. The data represented here is the mean of three experimental replicates with error bars showing ±SD.

Table 5
Processivity index of *Rf*GH5_4.

Reaction	Reducing Sugar (μg/mL) [R]	Reducing Ends in Insoluble Fraction (μg/mL) [I]	Processivity Index (PI) [R / I] *
Control	0.0	53.0	0.0
1 min	8.7	61.7	0.1
2 min	29.3	66.3	0.4
5 min	64.7	68.3	0.9
10 min	108.0	79.0	1.4
15 min	120.0	86.7	1.4
30 min	158.3	90.0	1.8
1 h	178.3	86.0	2.1
4 h	318.3	88.7	3.6
12 h	460.0	97.0	4.7
24 h	501.7	103.0	4.9

*Persistent increase in PI with time indicates processivity of *Rf*GH5_4.

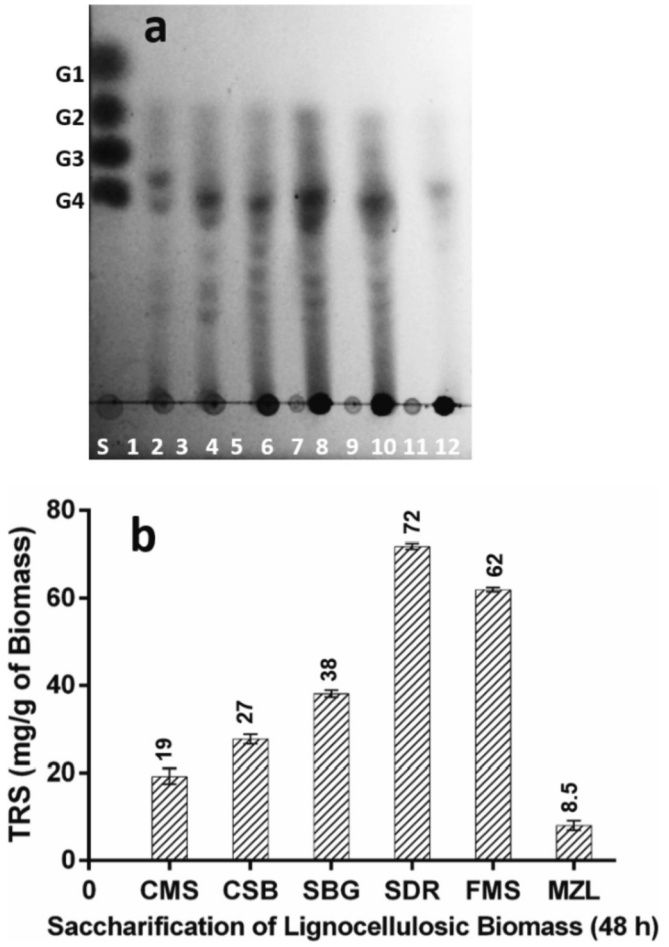

Fig. 6. The TLC analysis of hydrolysates (a) of pre-treated biomasses (cotton main stalk (CMS) and small branches (CSB), sugarcane bagasse (SBG), sorghum stalk (SDR), finger millet stalk (FMS) and maize leaves (MZL) generated by *Rf*GH5_4 in a 48 h saccharification experiment. Lanes S- Standard (G1, Glucose, G2, Cellobiose, G3, Cellotriose, G4, Cellotetraose), 1- Blank of CMS, 2- CMS, 3- Blank of CSB, 4- CSB, 5- Blank of SBG, 6- SBG, 7- Blank of SDR, 8- SDR, 9- Blank of FMS, 10- FMS, 11- Blank of MZL, 12-MZL. (b) TRS yield in mg/g of biomass, released by *Rf*GH5_4 from the various lignocellulosic biomasses was calculated. The saccharification experiment was run for 48 h at 30 °C, pH 5.5 of 20 mM citrate-phosphate buffer and 180 rpm. The data represented here is the mean of three experimental replicates with error bars showing ±SD.

stalk was saccharified by 100 U of commercial cellulase enzyme mixture at 50 °C for 72 h. The TRS obtained in the current study could be lower because, a lower biomass (pre-treated CMS or CSB) loading, 2% (w/v) was saccharified and for shorter period (48 h) using an in house produced single enzyme, endoglucanase (*Rf*GH5_4) at 30 °C which is a cost-effective process having lesser energy requirements. Moreover, all the TRS yields from the aforementioned reports were from the synergistic action of the three cellulases, namely endoglucanase, cellobiohydrolase and β-glucosidase, whereas the TRS from saccharification reported in present study is only by *Rf*GH5_4. Sorghum stalk and finger millet stalk were found to be the best lignocellulosic substrates for *Rf*GH5_4. Annual residual biomass of sorghum is estimated around 11 metric tons in India [27]. Finger millet is a drought tolerant rain-fed crop in India [28]. However, being a feed for livestock, these biomasses could be avoided for their use in renewable energy sector or could be used only after ensuring the food security of live stack. It is noteworthy that *Rf*GH5_4 hydrolyzed the cotton biomasses, CSB and CMS quite effectively. Cotton is an important cash crop worldwide having roughly 32-million-hectare area under cotton cultivation of which India accounts for about 10 million-hectares [25]. Farmers usually burn the biomass like cotton stalk after cotton plucking is complete. Cultivation of cotton generates abundant residual cotton biomass which could be used as a rich source of lignocellulose for bioethanol production. Thus, residual cotton stalk could be a good biomass resource for lignocellulosic bioethanol production. As a future prospect, efficient hydrolysis of cotton and other biomasses by synergistic action of *Rf*GH5_4 endoglucanase, cellobiohydrolase and β-glucosidase could overcome the bottleneck of getting less saccharification yield. Being a stable endoglucanase at 30 °C as discussed in Section 3.4, the saccharification reaction could be stretched for more than 96 h thus giving more yield of glucose. *Rf*GH5_4 endoglucanase hydrolysed various biomasses giving cellobiose (DP2) along with cellooligosaccharides of higher DP (DP3 and above) as observed in TLC analysis after 48 h of saccharification (Fig. 6 a). Therefore, *Rf*GH5_4 endoglucanase not only reduces the need of cellobiohydrolase to generate cellobiose during synergistic saccharification but it will also boost the saccharification process even if an additional cellobiohydrolase is used. *Rf*GH5_4 could also be immobilized using metal ion assisted recyclable pH-responsive polymer like Eudragit S100 to hydrolyse lignocellulose in bioethanol industry [55]. Moreover, *Rf*GH5_4 is sufficiently capable of hydrolysing hemicellulosic polysaccharides as described in Section 3.5.2 which further decreases the requirement of additional hemicellulases. Overall, this study affirms that *Rf*GH5_4 could potentially serve the lignocellulose conversion industry as a multifunctional yet an efficient processive endoglucanase.

This study established *Rf*GH5_4 as an efficient yet multifunctional endoglucanase. *Rf*GH5_4 was found to be hydrolysing both cellulosic and hemicellulosic polysaccharides. It gave maximum activity at pH 5.5 and 55 °C and was stable in pH range, 5.0–8.0 and between, 5 °C -45 °C.

Its catalytic efficiency against CMC-Na and konjac glucomannan was significantly superior to earlier reported endoglucanases. The melting temperature (T_m) of *Rf*GH5_4 was 70 °C, that was unaffected by EDTA or EGTA, indicating the absence of inherent divalent metal ions in the *Rf*GH5_4 structure. TLC and MALDI-TOF MS analyses of *Rf*GH5_4 treated hydrolysates of various polysaccharides showed presence of respective oligosaccharides (DP2-DP11) revealing the *endo*- and multi-ligand activity of the enzyme. *Rf*GH5_4 hydrolysed PASC processively thus generating cellobiose along with cellotriose thereby reducing the need of cellobiohydrolase. The efficient deconstruction and saccharification of various complex lignocellulosic biomasses was achieved using *Rf*GH5_4, which prospects it as a potential endoglucanase for the purpose of bioethanol production. The efficiency, multifunctionality, remarkable stability in ethanol, suitability for SSF and capability to hydrolyse a diverse range of lignocellulosic biomasses puts *Rf*GH5_4 in the category of cellulases important for renewable energy sector. The multifunctionality of *Rf*GH5_4 could be further explored for generation of various carbohydrate oligosaccharides useful in feed, food, prebiotics and health sector.

Abbreviations

EC	Enzyme Commission
HEC	Hydroxyethyl cellulose
CMC-Na	Carboxymethyl cellulose
IMAC	Immobilized Metal-ion Affinity Chromatography
pHTP1	Plasmid High-Throughput1
SDS	Sodium Dodecyl Sulphate
MES	2-(*N*-morpholino) ethane sulfonic acid
DMSO	Dimethyl Sulphoxide
DP	Degree of Polymerization
LB	Luria-Bertani
SSF	Simultaneous Saccharification and Fermentation
HPLC	High Pressure Liquid Chromatography
TRS	Total Reducing Sugar
XyGs	Xyloglucan Oligosaccharides
CMS	Cotton Main Stalk
CSB	Cotton Small Branches
SBG	Sugarcane Bagasse
SDR	*Sorghum Durra* Stalk
FMS	Finger Millet Stalk
MZL	Maize Leaves
μRIU	Micro Refractive Index Unit

CRediT authorship contribution statement

Parmeshwar Vitthal Gavande: Methodology, Investigation, Visualization, Software, Data Curation, Formal analysis, Validation, Writing-Original Draft Preparation, Rewriting and Editing. **Arun Goyal**: Conceptualization, Supervision, Resources, Project Administration, Rewriting, Editing. **Priyanka Nath**: Methodology, Reviewing. **Krishan Kumar:** Methodology, Reviewing. **Nazneen Ahmed:** Methodology. **Carlos M.G.A. Fontes:** Conceptualization, Methodology, Reviewing.

Declaration of competing interest

CMGAF is a financial beneficiary of the company that sells both the cloning kits used in this study and the enzyme that is described in this paper.

Acknowledgments

The research work was supported by a Trilateral project with the Indian Institute of Technology Bombay, Mumbai, India and All India Institute of Medical Sciences (AIIMS), New Delhi, India under the NERBPMC DBT-Twinning project scheme with the grant (No. BT/PR24786/NER/95/853/2017) from Department of Biotechnology, Ministry of Science and Technology, New Delhi, Government of India to AG. The authors are thankful to Central Instrumentation Facility (CIF), IIT Guwahati, for providing the MALDI-TOF MS facility. PVG and KK are grateful to the Ministry of Human Resource Development (MHRD), Govt. of India, for the fellowship. PN is thankful to the Department of Science and Technology (DST), Govt. of India, for the INSPIRE fellowship.

Ethical statement

This study does not contain any data generated using the participation of humans and other animals.

Appendix A. Supplementary data

Supplementary data to this article can be found online at https://doi.org/10.1016/j.ijbiomac.2022.04.059.

References

[1] S. Singh, A. Dhillon, A. Goyal, Enhanced catalytic efficiency of Bacillus amyloliquefaciens SS35 endoglucanase by ultraviolet directed evolution and mutation analysis, Renew. Energy 151 (2020) 1124–1133, https://doi.org/10.1016/j.renene.2019.11.105.

[2] K. Kumar, S. Singal, A. Goyal, Role of carbohydrate binding module (CBM3c) of GH9 β-1, 4 endoglucanase (Cel9W) from Hungateiclostridium thermocellum ATCC 27405 in catalysis, Carbohydr. Res. 484 (2019), 107782, https://doi.org/10.1016/j.carres.2019.107782.

[3] P. Liu, A. Li, Y. Wang, Q. Cai, H. Yu, Y. Li, H. Peng, Q. Li, Y. Wang, X. Wei, R. Zhang, Distinct miscanthus lignocellulose improves fungus secreting cellulases and xylanases for consistently enhanced biomass saccharification of diverse bioenergy crops, Renew. Energy 174 (2021) 799–809, https://doi.org/10.1016/j.renene.2021.04.107.

[4] L.R. Lynd, P.J. Weimer, W.H. Van Zyl, I.S. Pretorius, Microbial cellulose utilization: fundamentals and biotechnology, Microbiol. Mol. Biol. Rev. 66 (3) (2002) 506–577, https://doi.org/10.1128/mmbr.66.3.506-577.2002.

[5] V. Lombard, H.Golaconda Ramulu, E. Drula, P.M. Coutinho, B. Henrissat, The carbohydrate-active enzymes database (CAZy) in 2013, Nucleic Acid Res. 42 (D1) (2014) D490–D495, https://doi.org/10.1093/nar/gkt1178.

[6] H. Aspeborg, P.M. Coutinho, Y. Wang, H. Brumer, B. Henrissat, Evolution, substrate specificity and subfamily classification of glycoside hydrolase family 5 (GH5), BMC Evol. Biol. 12 (1) (2012) 186, https://doi.org/10.1186/1471-2148-12-186.

[7] R. Cheng, L. Cheng, L. Wang, R. Fu, X. Sun, J. Li, Characterization of an alkali-stable xyloglucanase/mixed-linkage β-glucanase Pgl5A from Paenibacillus sp. S09, Int. J. Biol. Macromol. 140 (2019) 1158–1166, https://doi.org/10.1016/j.ijbiomac.2019.08.210.

[8] Y.R. Yin, T. Li, P. Sang, R.F. Yang, H.Y. Liu, M. Xiao, S. Li, L.Q. Yang, W.J. Li, Characterization of an alkali-tolerant, thermostable, and multifunctional GH5 family endoglucanase from Thermoactinospora rubra YIM 77501T for prebiotic production, Biomass Convers. Biorefin. (2020) 1–10, https://doi.org/10.1007/s13399-020-00848-1.

[9] F. Zheng, J.V. Vermaas, J. Zheng, Y. Wang, T. Tu, X. Wang, X. Xie, B. Yao, G. T. Beckham, H. Luo, Activity and thermostability of GH5 endoglucanase chimeras from mesophilic and thermophilic parents, Appl. Environ. Microbiol. 85 (5) (2019), e02079-18, https://doi.org/10.1128/AEM.02079-18.

[10] A. Wierzbicka-Woś, R. Henneberger, R.A. Batista-García, L. Martínez-Ávila, S. A. Jackson, J. Kennedy, Biochemical characterization of a novel monospecific endo-β-1, 4-glucanase belonging to GH family 5 from a rhizosphere metagenomic library, Front. Microbiol. 10 (2019) 1342, https://doi.org/10.3389/fmicb.2019.01342.

[11] P.V. Gavande, A. Basak, S. Sen, K. Lepcha, N. Murmu, V. Rai, S. Saha, D. Muzumdar, V. Das, S. Ghosh, Functional characterization of thermotolerant microbial consortium for lignocellulolytic enzymes with central role of Firmicutes in rice straw depolymerisation, Sci. Rep. 11 (1) (2021) 1–13, https://doi.org/10.1038/s41598-021-82163-x.

[12] M.P. Bryant, N. Small, C. Bouma, I.M. Robinson, Characteristics of ruminal anaerobic cellulolytic cocci and Cillobacterium cellulosolvens n. sp, J. Bacteriol. 76 (5) (1958) 529–537, https://doi.org/10.1128/jb.76.5.529-537.1958.

[13] I. Venditto, A.S. Luis, M. Rydahl, J. Schückel, V.O. Fernandes, S. Vidal-Melgosa, P. Bule, A. Goyal, V.M.R. Pires, C.G. Dourado, Complexity of the Ruminococcus flavefaciens cellulosome reflects an expansion in glycan recognition, Proc. Natl. Acad. Sci. U. S. A. 113 (26) (2016) 7136–7141, https://doi.org/10.1073/pnas.1601558113.

[14] M.T. Rincon, B. Dassa, H.J. Flint, A.J. Travis, S. Jindou, I. Borovok, R. Lamed, E. Bayer, B. Henrissat, P.M. Coutinho, Abundance and diversity of dockerin-containing proteins in the fiber-degrading rumen bacterium, Ruminococcus flavefaciens FD-1, PLoS One 5 (8) (2010), e12476, https://doi.org/10.1371/journal.pone.0012476.

[15] D. Goyal, K. Kumar, M.S. Centeno, A. Thakur, V.M. Pires, P. Bule, C.M.G.A. Fontes, A. Goyal, Molecular cloning, expression and biochemical characterization of a family 5 glycoside hydrolase first endo-mannanase (RfGH5_7) from Ruminococcus flavefaciens FD-1 v3, Mol. Biotechnol. 61 (11) (2019) 826–835, https://doi.org/10.1007/s12033-019-00205-2.
[16] G.M. Boratyn, C. Camacho, P.S. Cooper, G. Coulouris, A. Fong, N. Ma, T.L. Madden, W.T. Matten, S.D. McGinnis, Y. Merezhuk, Y. Raytselis, BLAST: a more efficient report with usability improvements, Nucleic Acid Res. 41 (W1) (2013) W29–W33, https://doi.org/10.1093/nar/gkt282.
[17] P. Nath, A. Dhillon, K. Kumar, K. Sharma, S.B. Jamaldheen, V.S. Moholkar, A. Goyal, Development of bi-functional chimeric enzyme (CtGH1-L1-CtGH5-F194A) from endoglucanase (CtGH5) mutant F194A and β-1, 4-glucosidase (CtGH1) from Clostridium thermocellum with enhanced activity and structural integrity, Bioresour. Technol. 282 (2019) 494–501, https://doi.org/10.1016/j.biortech.2019.03.051.
[18] Y.H.P. Zhang, J. Cui, L.R. Lynd, L.R. Kuang, A transition from cellulose swelling to cellulose dissolution by o-phosphoric acid: evidence from enzymatic hydrolysis and supramolecular structure, Biomacromolecules 7 (2) (2006) 644–648, https://doi.org/10.1021/bm050799c.
[19] N. Nelson, A photometric adaptation of the Somogyi method for the determination of glucose, J. Biol. Chem. 153 (2) (1944) 375–380.
[20] M. Somogyi, A new reagent for the determination of sugars, J. Biol. Chem. 160 (1945) 61–68, https://doi.org/10.1016/S0021-9258(18)43098-0.
[21] K. Sharma, I.L. Antunes, V. Rajulapati, A. Goyal, Molecular characterization of a first endo-acting β-1,4-xylanase of family 10 glycoside hydrolase (PsGH10A) from Pseudopedobacter saltans comb. nov, Process Biochem. 70 (2018) 79–89, https://doi.org/10.1016/j.procbio.2018.03.025.
[22] H. Lineweaver, D. Burk, The determination of enzyme dissociation constants, J. Am. Chem. Soc. 56 (3) (1934) 658–666.
[23] L. Michaelis, M. Menten, Die kinetik der invertinwirkung, Biochemistry 49 (1913) 333–369, https://doi.org/10.1021/bi201284u.
[24] J. Son, S. Cha, MALDI mass spectrometric analysis of nonderivatized steroids using cyclodextrin-supported 2, 5-dihydroxybenzoic acid as matrix, Bull. Kor. Chem. Soc. 35 (5) (2014) 1409–1412, https://doi.org/10.5012/bkcs.2014.35.5.1409.
[25] M.Z. Baig, S.M. Dharmadhikari, Bioethanol production from enzymatically hydrolysed cotton stalk: one approach towards sustainable energy development, Curr. World Environ. 9 (3) (2014) 940, https://doi.org/10.12944/CWE.9.3.46.
[26] Z. Talha, W. Ding, E. Mehryar, M. Hassan, J. Bi, Alkaline pretreatment of sugarcane bagasse and filter mud codigested to improve biomethane production, Biomed. Res. Int. (2016) 1–10, https://doi.org/10.1155/2016/8650597.
[27] S.B. Jamaldheen, K. Sharma, A. Rani, V.S. Moholkar, A. Goyal, Comparative analysis of pretreatment methods on sorghum (Sorghum durra) stalk agrowaste for holocellulose content, Prep. Biochem. Biotechnol. 48 (6) (2018) 457–464, https://doi.org/10.1080/10826068.2018.1466148.
[28] S.B. Jamaldheen, A. Thakur, V.S. Moholkar, A. Goyal, Enzymatic hydrolysis of hemicellulose from pre-treated Finger millet (Eleusine coracana) straw by recombinant endo-1,4-β-xylanase and exo-1, 4-β-xylosidase, Int. J. Biol. Macromol. 135 (2019) 1098–1106, https://doi.org/10.1016/j.ijbiomac.2019.06.010.
[29] M. Madadi, Y. Tu, A. Abbas, Recent status on enzymatic saccharification of lignocellulosic biomass for bioethanol production, Electron J. Biol. 13 (2) (2017) 135–143.
[30] M.E.B. Miller, D.A. Antonopoulos, M.T. Rincon, M. Band, A. Bari, T. Akraiko, A. Hernandez, J. Thimmapuram, B. Henrissat, P.M. Coutinho, Diversity and strain specificity of plant cell wall degrading enzymes revealed by the draft genome of Ruminococcus flavefaciens FD-1, PLoS One 4 (8) (2009), https://doi.org/10.1371/journal.pone.0006650.
[31] F. Foong, R. Doi, Characterization and comparison of Clostridium cellulovorans endoglucanases-xylanases EngB and EngD hyperexpressed in Escherichia coli, J. Bacteriol. 174 (4) (1992) 1403–1409, https://doi.org/10.1128/jb.174.4.1403-1409.1992.
[32] M. Barros, J. Thomson, Cloning and expression in Escherichia coli of a cellulase gene from Ruminococcus flavefaciens, J. Bacteriol. 169 (4) (1987) 1760–1762, https://doi.org/10.1128/jb.169.4.1760-1762.1987.
[33] A.O. Lima, M.C. Quecine, M.H. Fungaro, F.D. Andreote, W. Maccheroni, W. L. Araújo, M. Silva-Filho, C. Marcio, A. Pizzirani-Kleiner, A. Aline, J.L. Azevedo, Molecular characterization of a β-1, 4-endoglucanase from an endophytic Bacillus pumilus strain, Appl. Microbiol. Biotechnol. 68 (1) (2005) 57–65, https://doi.org/10.1007/s00253-004-1740-1.
[34] E.M. Glasgow, E.I. Kemna, C.A. Bingman, N. Ing, K. Deng, C.M. Bianchetti, T. E. Takasuka, T.R. Northen, B.G. Fox, A structural and kinetic survey of GH5_4 endoglucanases reveals determinants of broad substrate specificity and opportunities for biomass hydrolysis, J. Biol. Chem. 295 (51) (2020) 17752–17769, https://doi.org/10.1074/jbc.ra120.015328.
[35] R. Rashmi, K. Siddalingamurthy, Microbial xyloglucanases: a comprehensive review, Biocatal. Biotransform. 36 (4) (2018) 280–295, https://doi.org/10.1080/10242422.2017.1417394.
[36] J. Larsen, M.Østergaard Petersen, L. Thirup, H.Wen Li, F.Krogh Iversen, The IBUS process–lignocellulosic bioethanol close to a commercial reality, Chem. Eng. Technol. 31 (5) (2008) 765–772, https://doi.org/10.1002/ceat.200800048.
[37] H. Kui, H. Luo, P. Shi, Y. Bai, T. Yuan, Y. Wang, P. Yang, S. Dong, B. Yao, Gene cloning, expression, and characterization of a thermostable xylanase from Nesterenkonia xinjiangensis CCTCC AA001025, Appl. Biochem. Biotechnol. 162 (4) (2010) 953–965, https://doi.org/10.1007/s12010-009-8815-5.
[38] D.W. Gohara, E. Di Cera, Molecular mechanisms of enzyme activation by monovalent cations, J. Biol. Chem. 291 (40) (2016) 20840–20848, https://doi.org/10.1074/jbc.r116.737833.
[39] Y.H. Li, M. Ding, J. Wang, G.J. Xu, F. Zhao, A novel thermoacidophilic endoglucanase, Ba-EGA, from a new cellulose-degrading bacterium, Bacillus sp. AC-1, Appl. Microbiol. Biotechnol. 70 (4) (2006) 430–436, https://doi.org/10.1007/s00253-005-0075-x.
[40] G.S. Naika, P.K. Tiku, Influence of ethylenediaminetetraacetic acid (EDTA) on the structural stability of endoglucanase from Aspergillus aculeatus, J. Agric. Food Chem. 59 (13) (2011) 7341–7345, https://doi.org/10.1021/jf103889m.
[41] C.M. Lee, Y.S. Lee, S.H. Seo, S.H. Yoon, S.J. Kim, B.S. Hahn, J.S. Sim, B.S. Koo, Screening and characterization of a novel cellulase gene from the gut microflora of Hermetia illucens using metagenomic library, J. Microbiol. Biotechnol. 24 (9) (2014) 1196–1206, https://doi.org/10.4014/jmb.1405.05001.
[42] O.R. Adeoyo, B.I. Pletschke, J.F. Dames, Improved endoglucanase production and mycelial biomass of some ericoid fungi, AMB Express 7 (1) (2017) 1–8, https://doi.org/10.1186/s13568-016-0312-y.
[43] H. Nakazawa, K. Okada, R. Kobayashi, T. Kubota, T. Onodera, N. Ochiai, N. Omata, W. Ogasawara, H. Okada, Y. Morikawa, Characterization of the catalytic domains of Trichoderma reesei endoglucanase I, II, and III, expressed in Escherichia coli, Appl. Microbiol. Biotechnol. 81 (4) (2008) 81–689, https://doi.org/10.1007/s00253-008-1667-z.
[44] H. Nakazawa, K. Okada, T. Onodera, W. Ogasawara, H. Okada, Y. Morikawa, Directed evolution of endoglucanase III (Cel12A) from Trichoderma reesei, Appl. Microbiol. Biotechnol. 83 (4) (2009) 649–657, https://doi.org/10.1007/s00253-009-1901-3.
[45] S.F. Yuan, T.H. Wu, H.L. Lee, H.Y. Hsieh, W.L. Lin, B. Yang, C.K. Chang, Q. Li, J. Gao, C.H. Huang, Biochemical characterization and structural analysis of a bifunctional cellulase/xylanase from Clostridium thermocellum, J. Biol. Chem. 290 (9) (2015) 5739–5748, https://doi.org/10.1074/jbc.m114.604454.
[46] B. Wu, S. Zheng, M.M. Pedroso, L.W. Guddat, S. Chang, B. He, G. Schenk, Processivity and enzymatic mechanism of a multifunctional family 5 endoglucanase from Bacillus subtilis BS-5 with potential applications in the saccharification of cellulosic substrates, Biotechnol. Biofuels. 11 (1) (2018) 1–15, https://doi.org/10.1186/s13068-018-1022-2.
[47] K. Lv, W. Shao, M.M. Pedroso, J. Peng, B. Wu, J. Li, B. He, G. Schenk, Enhancing the catalytic activity of a GH5 processive endoglucanase from Bacillus subtilis BS-5 by site-directed mutagenesis, Int. J. Biol. Macromol. 168 (2021) 442–452, https://doi.org/10.1016/j.ijbiomac.2020.12.060.
[48] L.P. Meleiro, S. Carli, R. Fonseca-Maldonado, M. da Silva Torricillas, A.L.R. L. Zimbardi, R.J. Ward, J.A. Jorge, A. Joao, R.P.M. Furriel, Overexpression of a cellobiose-glucose-halotolerant endoglucanase from Scytalidium thermophilum, Appl. Biochem. Biotechnol. 185 (1) (2018) 316–333, https://doi.org/10.1007/s12010-017-2660-8.
[49] P. Phadtare, S. Joshi, T. Satyanarayana, Recombinant thermo-alkali-stable endoglucanase of Myceliopthora thermophila BJA (rMt-egl): biochemical characteristics and applicability in enzymatic saccharification of agro-residues, Int. J. Biol. Macromol. 104 (2017) 107–116, https://doi.org/10.1016/j.ijbiomac.2017.05.167.
[50] X.M. Huang, Q.Q. Li, X.L. Chen, J.X. Fan, X.H. Xu, X.D. Sun, D.Y. Li, H.X. Zhao, Expression and characteristics of an endoglucanase from Trichoderma atroviride (TaEGII) in Saccharomyces cerevisiae, Appl. Biochem. Biotechnol. 182 (3) (2017) 1158–1170, https://doi.org/10.1007/s12010-016-2389-9.
[51] K. Yaoi, T. Nakai, Y. Kameda, A. Hiyoshi, Y. Mitsuishi, Cloning and characterization of two xyloglucanases from Paenibacillus sp. strain KM21, Appl. Environ. Microbiol. 71 (12) (2005) 7670–7678, https://doi.org/10.1128/aem.71.12.7670-7678.2005.
[52] A. Bala, B. Singh, Cellulolytic and xylanolytic enzymes of thermophiles for the production of renewable biofuels, Renew. Energy 136 (2019) 1231–1244, https://doi.org/10.1016/j.renene.2018.09.100.
[53] F. Zheng, S. Ding, Processivity and enzymatic mode of a glycoside hydrolase family 5 endoglucanase from Volvariella volvacea, Appl. Environ. Microbiol. 79 (3) (2013) 989–996, https://doi.org/10.1128/aem.02725-12.
[54] P. Nath, P.D. Maibam, S. Singh, V. Rajulapati, A. Goyal, Sequential pretreatment of sugarcane bagasse by alkali and organosolv for improved delignification and cellulose saccharification by chimera and cellobiohydrolase for bioethanol production, 3 Biotech 11 (2) (2021) 1–16, https://doi.org/10.1007/s13205-020-02600-y.
[55] K. Lv, Z. Yu, M.M. Pedroso, B. Wu, Z. Gao, B. He, G. Schenk, Metal affinity immobilization of the processive endoglucanase EG5C-1 from Bacillus subtilis on a recyclable pH-responsive polymer, ACS Sustain. Chem. Eng. 11 (21) (2021) 1–15, https://doi.org/10.1021/acssuschemeng.1c02215.